

University of Windsor

## Scholarship at UWindor

---

Electronic Theses and Dissertations

Theses, Dissertations, and Major Papers

---

2009

# Rate of growth and dissipation of queue on freeways and its effect on crash likelihood

Steven Volpatti  
*University of Windsor*

Follow this and additional works at: <https://scholar.uwindsor.ca/etd>

---

### Recommended Citation

Volpatti, Steven, "Rate of growth and dissipation of queue on freeways and its effect on crash likelihood" (2009). *Electronic Theses and Dissertations*. 8231.  
<https://scholar.uwindsor.ca/etd/8231>

This online database contains the full-text of PhD dissertations and Masters' theses of University of Windsor students from 1954 forward. These documents are made available for personal study and research purposes only, in accordance with the Canadian Copyright Act and the Creative Commons license—CC BY-NC-ND (Attribution, Non-Commercial, No Derivative Works). Under this license, works must always be attributed to the copyright holder (original author), cannot be used for any commercial purposes, and may not be altered. Any other use would require the permission of the copyright holder. Students may inquire about withdrawing their dissertation and/or thesis from this database. For additional inquiries, please contact the repository administrator via email ([scholarship@uwindsor.ca](mailto:scholarship@uwindsor.ca)) or by telephone at 519-253-3000ext. 3208.

**RATE OF GROWTH AND DISSIPATION OF QUEUE ON FREEWAYS  
AND ITS EFFECT ON CRASH LIKELIHOOD**

By

Steven Volpatti

A Thesis

Submitted to the Faculty of Graduate Studies through Civil  
and Environmental Engineering in Partial Fulfillment  
of the Requirements for the Degree of  
Master of Applied Science at the  
University of Windsor

Windsor, Ontario, Canada

2009

© 2009 Steven Volpatti



Library and Archives  
Canada

Published Heritage  
Branch

395 Wellington Street  
Ottawa ON K1A 0N4  
Canada

Bibliothèque et  
Archives Canada

Direction du  
Patrimoine de l'édition

395, rue Wellington  
Ottawa ON K1A 0N4  
Canada

*Your file* *Votre référence*  
ISBN: 978-0-494-57632-8  
*Our file* *Notre référence*  
ISBN: 978-0-494-57632-8

**NOTICE:**

The author has granted a non-exclusive license allowing Library and Archives Canada to reproduce, publish, archive, preserve, conserve, communicate to the public by telecommunication or on the Internet, loan, distribute and sell theses worldwide, for commercial or non-commercial purposes, in microform, paper, electronic and/or any other formats.

The author retains copyright ownership and moral rights in this thesis. Neither the thesis nor substantial extracts from it may be printed or otherwise reproduced without the author's permission.

**AVIS:**

L'auteur a accordé une licence non exclusive permettant à la Bibliothèque et Archives Canada de reproduire, publier, archiver, sauvegarder, conserver, transmettre au public par télécommunication ou par l'Internet, prêter, distribuer et vendre des thèses partout dans le monde, à des fins commerciales ou autres, sur support microforme, papier, électronique et/ou autres formats.

L'auteur conserve la propriété du droit d'auteur et des droits moraux qui protègent cette thèse. Ni la thèse ni des extraits substantiels de celle-ci ne doivent être imprimés ou autrement reproduits sans son autorisation.

---

In compliance with the Canadian Privacy Act some supporting forms may have been removed from this thesis.

While these forms may be included in the document page count, their removal does not represent any loss of content from the thesis.

Conformément à la loi canadienne sur la protection de la vie privée, quelques formulaires secondaires ont été enlevés de cette thèse.

Bien que ces formulaires aient inclus dans la pagination, il n'y aura aucun contenu manquant.

  
**Canada**

## DECLARATION OF PREVIOUS PUBLICATION

This thesis includes material from one original paper that has been previously submitted for publication in a peer reviewed journal, as follows:

Lee, C. and Volpatti, S. (2009). *Effects of Shock Waves on Freeway Crash Likelihood*. Submitted for presentation at the 89<sup>th</sup> Transportation Research Board Annual Meeting and publication in the Transportation Research Record. Washington, D.C., 19 pages.

I certify that I have obtained a written permission from the copyright owner(s) to include the above published material(s) in my thesis. I certify that the above material describes work completed during my registration as graduate student at the University of Windsor.

I declare that, to the best of my knowledge, my thesis does not infringe upon anyone's copyright nor violate any proprietary rights and that any ideas, techniques, quotations, or any other material from the work of other people included in my thesis, published or otherwise, are fully acknowledged in accordance with the standard referencing practices. Furthermore, to the extent that I have included copyrighted material that surpasses the bounds of fair dealing within the meaning of the Canada Copyright Act, I certify that I have obtained a written permission from the copyright owner(s) to include such material(s) in my thesis.

I declare that this is a true copy of my thesis, including any final revisions, as approved by my thesis committee and the Graduate Studies office, and that this thesis has not been submitted for a higher degree to any other University or Institution.

## ABSTRACT

To improve traffic safety on freeways, many traffic researchers have used real time data to predict the likelihood of crashes, using number of crashes as the measure of safety. The parameters of speed, volume or density have been used extensively in previous research to calculate the crash likelihood.

This research studied the combined effects of volume and density to predict crash likelihood using real time data a short time before crash occurrence. The volume-density relationship provided a measure of growth and dissipation of queue on the freeway, known as the shock wave speed. Using this shock wave speed and quantifying various types of shock waves, analysis was done to predict crash likelihood.

The results of logistic regression analysis indicated that increasing the speed of forward shock wave decrease crash likelihood. Using a log-linear relationship and including exposure measures, it was found that diverging sections, normal weather conditions, low shock wave speeds and forward moving shock waves indicated increased likelihood of crashes. Finally, using an odds ratio to compare the combined effects of shock wave speed and shock wave type, it was determined that forward moving shock waves yield a greater likelihood of crash for both low and high shock wave speeds.

***To my parents, Faustino and Franca Volpatti and my sisters Angela and Diana***

## ACKNOWLEDGEMENTS

I would like to take this opportunity to sincerely thank my supervisor, Dr. Chris Lee, for his continued support, assistance, guidance, and constructive evaluations throughout the course of my thesis project. I truly appreciate the confidence he has shown in me and have learned a great deal working with him. I would also like to thank my evaluation committee of Dr. Faouzi Ghrib, Dr. Guoqing Zhang, Dr. Sreekanta Das and special committee member, Mr. John Tofflemire, for their suggestions to improve this thesis. I would like to send a special thank you to Mr. Tofflemire, who introduced me to traffic and transportation engineering.

I would also like to express thanks to my friends as well as colleagues at the University, especially Benjamin Hodi, Thomas Ring, Sara Kenno, Adam Mourad and James Bryant, who have lent their support and expertise throughout the course of this project.

A heartfelt thank you goes out to Dr. N.K. Becker. Dr. Becker first introduced me to civil engineering and has always been available to help with any concerns I may have had throughout my studies. He has always been supportive of me and challenged me to strive for the top.

Lastly, I would like to thank my parents, Faustino and Franca and my two sisters, Angela and Diana, for their continued encouragement, support and belief in me throughout the course of my studies.

## TABLE OF CONTENTS

DECLARATION PREVIOUS PUBLICATION.....	iii
ABSTRACT.....	iv
ACKNOWLEDGEMENTS.....	vi
LIST OF TABLES.....	ix
LIST OF FIGURES.....	x
NOMENCLATURE.....	xi
1 INTRODUCTION .....	1
1.1 Overview.....	1
1.2 Research Objectives .....	2
1.3 Organization of Thesis .....	2
2 LITERATURE REVIEW.....	3
2.1 Traffic Flow Theory .....	3
2.2 Shock wave Theory.....	7
2.3 Real-Time Crash Analysis.....	8
2.4 Evaluation of Literature .....	12
3 DATA .....	14
3.1 Traffic Data .....	14
3.2 Incident Logs.....	15
3.3 Weather Data .....	16
3.4 Exposure .....	17
4 PROCEDURE.....	19
4.1 Classification of Shock waves .....	19
4.2 Critical Values and Trends .....	20
4.3 Determining Shock wave.....	24
4.4 Effect of Ramps on Mainline Traffic .....	27
4.5 Statistical Analysis Techniques .....	27
4.5.1 Logistic Regression Model.....	28
4.5.2 Log Linear Model .....	28
5 RESULTS AND ANALYSIS .....	32
5.1 Shock waves .....	32
5.2 Effect of Ramps on Mainline Traffic .....	40



5.3	Ideal Time Period.....	41
5.4	Logistic Regression Model.....	41
5.5	Log linear Model.....	43
6	CONCLUSIONS AND RECOMMENDATIONS .....	50
6.1	Conclusions.....	50
6.2	Recommendations.....	51
	REFERENCES .....	53
	APPENDIX A .....	55
	VITA AUCTORIS.....	66

## LIST OF TABLES

Table 3-1: Sample Raw Data .....	15
Table 3-2: Exposure for Each Road Section .....	18
Table 5-1: Shock waves Sorted by Shock wave Type (Crash Cases) .....	32
Table 5-2: Average Shock wave Speed by Type (Crash Cases) .....	34
Table 5-3: Shock waves by Shock wave Type (Non-Crash Cases) .....	35
Table 5-4: Average Shock wave Speed by Type (Non-Crash Cases) .....	37
Table 5-5: Results of Log Linear Model - Eastbound Lanes .....	45
Table 5-6: Results of Log Linear Model - Westbound Lanes .....	46
Table 5-7: Observed and Expected Frequencies.....	47
Table 5-8: Exposure Comparison – Westbound Lanes .....	48
Table 5-9: Log-odds Ratio - Westbound Lanes .....	49

## LIST OF FIGURES

Figure 2.1: Time Space Diagram of Vehicle Trajectory .....	4
Figure 2.2: Volume-Density Relationship .....	5
Figure 2.3: Speed-Volume Relationship.....	6
Figure 2.4: Speed-Density Relationship .....	7
Figure 2.5: Calculating Shock Wave Speed .....	8
Figure 3.1: Detector Location on the Gardiner Expressway .....	14
Figure 3.2: Speed Profile – Station 60.....	16
Figure 4.1: Shock wave Types .....	20
Figure 4.2: Volume-Density Graphs for Westbound Traffic.....	22
Figure 4.3 : Volume-Density Graphs for Eastbound Traffic .....	23
Figure 4.4: Shock wave Types .....	26
Figure 4.5: Averaging Points .....	27
Figure 5.1: Frequency of Crashes.....	38
Figure 5.2: Frequency of Crashes – Forward Shock waves.....	39
Figure 5.3: Frequency of Crashes– Backward Shock waves.....	40
Figure 5.4: Comparison of Ramp and Mainline Traffic Volumes .....	41

## NOMENCLATURE

exp	exposure (log-linear model)
$F_{ij}$	expected frequency for variable A with category i and variable B with category j (log-linear model)
$F_{ij}$	expected frequency of case (Log odds ratio)
$F_{1j}$	expected frequency of base case (Log odds ratio)
k	density of road section (veh/km)
$n_j$	observed frequency (Chi-Square Statistic)
$P_i(k)$	probability that frequency of event is (k=0, 1, 2, 3, ...) – (Poisson)
$P(Y = i)$	the probability of occurrence of a crash (logistic regression model)
q	volume of road section (veh/hr)
ShockSpeed	actual shock wave speed in km/hr
t	number of intervals (Poisson)
u	speed (km/hr)
$x_{ik}$	explanatory variable (logistic regression model)
$Y_i$	random variable of accident counts on entity i (Negative Binomial)
$y_i$	specific accident count on entity j (Negative Binomial)
$\alpha$	constant (logistic regression model)
$\beta_k$	coefficient for the explanatory variable (logistic regression model)
$\beta_{exp}$	coefficient of the exposure measure (log-linear model)
$\eta_i$	expected number of events (Negative Binomial)
$\theta$	constant (Log odds ratio)
$\lambda_i$	expected value of event frequency for ith interval (Poisson)
$\lambda_{GEOMETRY}$	coefficient for geometric condition (log linear model)

$\lambda_{\text{WEATHER}}$	coefficient for weather (log linear model)
$\lambda_{\text{SHOCKTYPE}}$	coefficient for shock wave type (log linear model)
$\lambda_{\text{SHOCKSPEED}}$	coefficient for shock wave speed (log linear model)
$\lambda_{\text{TYPESPEED}}$	coefficient for interaction between shock wave type and shock wave speed (log linear model)
$\lambda_{x(i)}, \lambda_{y(i)}$	coefficients for variables X and Y (Log odds ratio)
$\lambda_{xy(ij)}, \lambda_{xy(1j)}$	coefficient for interaction of variables X and Y (Log odds ratio)
$\lambda_{x(1)}$	coefficient for base case (Log odds ratio)
$\mu_j$	expected frequency (Chi-Square Statistic)
$\phi$	overdispersion parameter (Negative Binomial)
$\chi$	chi-squared statistic
$\omega_{AB}$	shock wave speed (km/hr)

# 1 INTRODUCTION

## 1.1 Overview

Over the last half century, the transportation industry has become an essential need for many people around the world, especially in North America, whether it is freight shipping for businesses or for one's personal use to travel to and from work. Due to increase in demand for trips by motor vehicle, the increased capacity of road is needed. Over the years, there have been significant advances in road design and traffic management to alleviate congestion and improve safety for travelers. Some of the road design and traffic management methods include enhancing road geometric conditions such as increased lane width, increased stretches of straight roadways, strengthened and reinforced pavements, increased and enhanced traffic signage, and intelligent traffic control.

Prior to any additions or upgrades to the road network, studies must be conducted to determine if there is a need for any changes, and how the changes will affect the current traffic situation in the study area. Safety can be measured in many ways; however it is commonly measured in terms of number and severity of crashes in the network.

Existing road networks are continually monitored by researchers and planners to identify the locations with high number of severe crashes. In more recent years, given that crashes tend to occur due to short term variation in traffic flow, traffic conditions have been monitored in real time. These real-time traffic flow parameters have been related to the potential of crash occurrence. With the adaptation of real-time traffic conditions, it is possible to predict the dangerous conditions in advance and prevent crashes. Research is focused on proactive approaches to prevent crashes rather than reactive measures. The goal of the research is to use

proactive approaches to determine whether or not a crash will occur based on the most up to date traffic conditions.

## 1.2 Research Objectives

The goals of this research are as follows:

1. To understand how a queue forms or dissipates in a short time period before a crash occurs.
2. To estimate the likelihood of crash occurrence – based on queue formation and dissipation.

## 1.3 Organization of Thesis

The thesis is organized in six chapters. Chapter 2 deals with literature review of traffic flow theory, shock wave theory, studies on real-time analysis of traffic data and the likelihood of crash risk and studies indicating the effects of shock wave speed on traffic flow. Chapter 3 describes the data used in this study. Chapter 4 covers the procedure used in the study. Chapter 5 presents results and analysis of the study. Chapter 6 includes the conclusions and recommends future research.

## 2 LITERATURE REVIEW

### 2.1 Traffic Flow Theory

Traffic flow theory explains interaction between vehicles and the roadway system. The theory was developed from physics and mathematics to explain the relationships of traffic stream parameters. Traffic stream parameters are classified as one of two broad categories: microscopic parameters and macroscopic parameters.

Microscopic parameters reflect the behaviour of individual vehicles in a traffic stream and the microscopic traffic flow models describe the behaviour of the car following. The parameters used for an individual vehicle are: spacing ( $s_i$ ), headway ( $h_i$ ) and speed ( $u_i$ ). The spacing is defined as the distance between two successive vehicles and has units of distance per vehicle. The headway is defined as the time between two successive vehicles, in the units of time per vehicle. The speed is the distance per unit time for each vehicle. The spacing, headway and speed can be measured using a time-space diagram of vehicle trajectory. In Figure 2.1, the spacing is the vertical distance between the vehicle's trajectories, whereas the headway is the horizontal distance between the vehicle's trajectories. The instantaneous speed is the slope of a line tangent to any point on the vehicle's path. The vehicle trajectories in the following figure indicate that the vehicles are not travelling at a constant speed given that the paths are not straight lines.



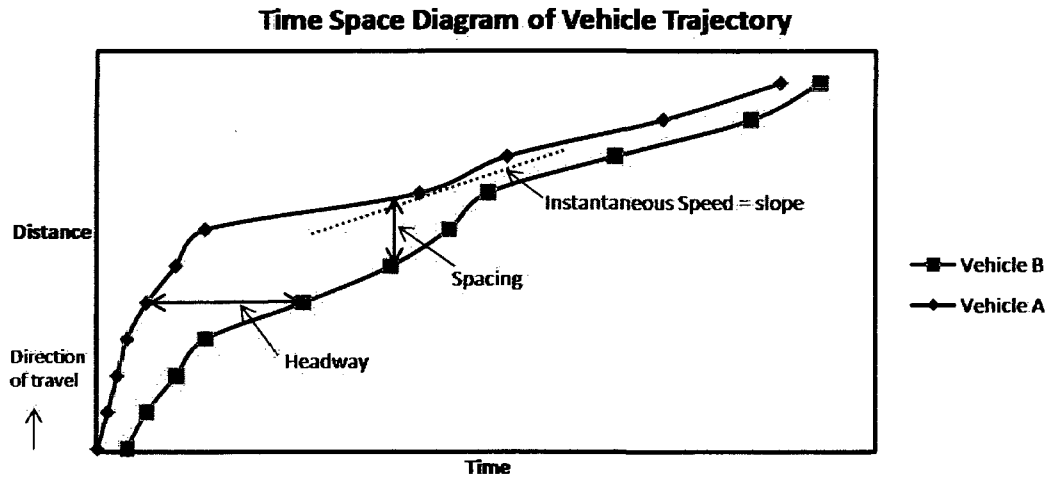


Figure 2.1: Time Space Diagram of Vehicle Trajectory

Macroscopic parameters are the average behaviour of a group of vehicles. The traffic flow models for these parameters describe the relationships among volume, speed and density. Volume ( $q$ ) is defined as the number of vehicles that pass through a given interval in a specified period and is typically measured in vehicles per hour. Density ( $k$ ) is the number of vehicles that pass a given length of road, usually recorded in vehicles per kilometre. These three parameters are interrelated in the following fundamental equation of traffic flow:

$$k = \frac{q}{u} \tag{1}$$

Given that it is very difficult to measure the density in the field, the density is usually calculated using this equation.

Traffic flow can be classified into two principle categories: 1) uninterrupted flow: flow of traffic is not disrupted by external factors (e.g. freeway flows), and 2) interrupted flow: traffic flow is disrupted periodically by external factors such as traffic signals or signage in the road network. Even if the freeway is in a congested state, it is still classified as uninterrupted flow due to the fact the disruption is not periodically disrupted by external factors.

For uninterrupted flow, the combinations of speed, volume and density are able to produce further two-dimensional relationships, which can be used to extract valuable information about the traffic flow in the area of interest. Figure 2.2 shows the relationship between volume and density, which forms an inverted parabolic shape. In this figure, the highest point of the parabola in the  $q$ -axis represents the capacity and the critical density of the roadway, with all values to the left of the point being in the uncongested state and all values to the right of this point being in the congested state. The capacity is the point in which the road network is considered to have reached its maximum number of vehicles per unit time. The point where the congested side of the parabola intersects with the  $k$ -axis is the jam density. The jam density is the maximum number of vehicles per unit distance, which occurs when volume is zero (i.e. all vehicles are stopped).

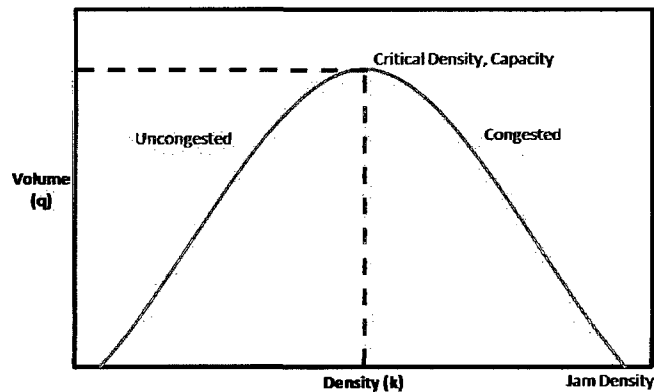


Figure 2.2: Volume-Density Relationship

The relationship between the speed and the volume also forms a parabolic relationship as shown in Figure 2.3. The highest point in the  $q$ -axis again represents the capacity of the roadway, and the speed at capacity is called the critical speed. This critical speed specifies the boundary between uncongested and congested flow. The uncongested flow is represented by the top portion of the graph (when the speed is greater than the critical speed) whereas the

congested flow is represented by the lower portion of the graph (when the speed is lower than the critical speed). The other important point from this graph is the free flow speed, which occurs when the volume is zero and the speed is maximum (highest point on the graph). Traffic engineers use this graph to find the level of service of a road network. The system assigns a grade based on the traffic flow from A to F, with A being the free flow speed, progressing along to E, which is the critical speed and capacity, and the congested phase, represented by level of service F. This is primarily used when determining what roads need to be upgraded within a system when a change occurs to increase the capacity of the road (e.g. new subdivision, new commercial centre, etc.).

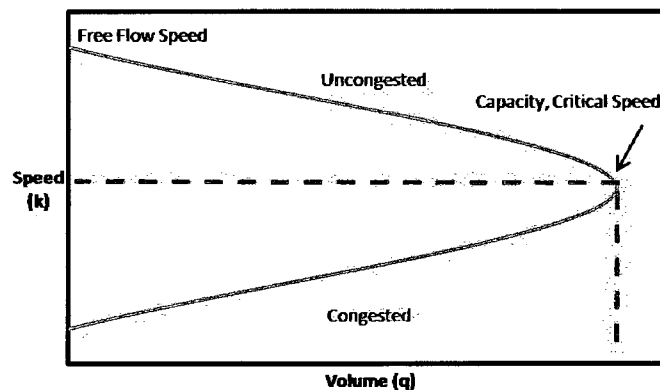


Figure 2.3: Speed-Volume Relationship

The third relationship is between speed and density is shown in Figure 2.4. The form of this may not necessarily be a straight line, but in general, speed and density simultaneously increase and decrease. From this graph, the free flow speed and the jam density can easily be obtained, using the intersection points of the u-axis and k-axis respectively for the values. There exists a transition point between uncongested and congested flow, specifically at the critical speed and critical density. However this point is unable to be determined directly from this graph.

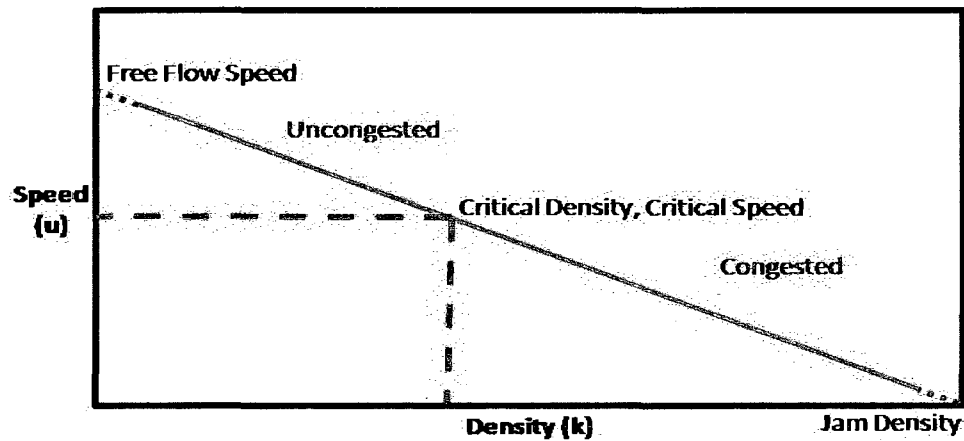


Figure 2.4: Speed-Density Relationship

As shown in the previous three figures, all three traffic flow parameters are closely related to each other. It should be noted that the volume itself cannot reflect the level of congestion due to the fact the same volume can occur for both uncongested and congested conditions. Another useful method of quantifying the level of congestion on the freeways is to investigate the effects of the rate of growth and congestion of queue on freeways. This is called shock wave analysis.

## 2.2 Shock wave Theory

Shock wave theory is a classical theory that was first derived by Richards (1956) and later developed by Lighthill and Whitham (1957). The traffic state is represented by flow and concentration of traffic (or density). Shock wave is defined as the change in volume (measured in veh/hour) divided by the change in density (measured in veh/km) between two traffic states. The speed of the shock wave is typically measured in km/hour. The equation of a shock wave represents the formula for the slope of a line as follows:

$$\omega_{AB} = \frac{\Delta q}{\Delta k} = \frac{q_A - q_B}{k_A - k_B} \quad (2)$$

Where,

$\omega_{AB}$  = speed of shock wave moving from traffic state A to traffic state B;  
 $q_A, q_B$  = volumes at traffic states A and B, respectively;

$k_A, k_B$  = densities at traffic states A and B, respectively.

Since the parameters for measuring shock wave speed are volume and density, the graphical relationship shown in Figure 2.5 can be used to calculate the speed of the shock wave. Shock wave theory is useful for quantifying the rate of growth or dissipation of queue.

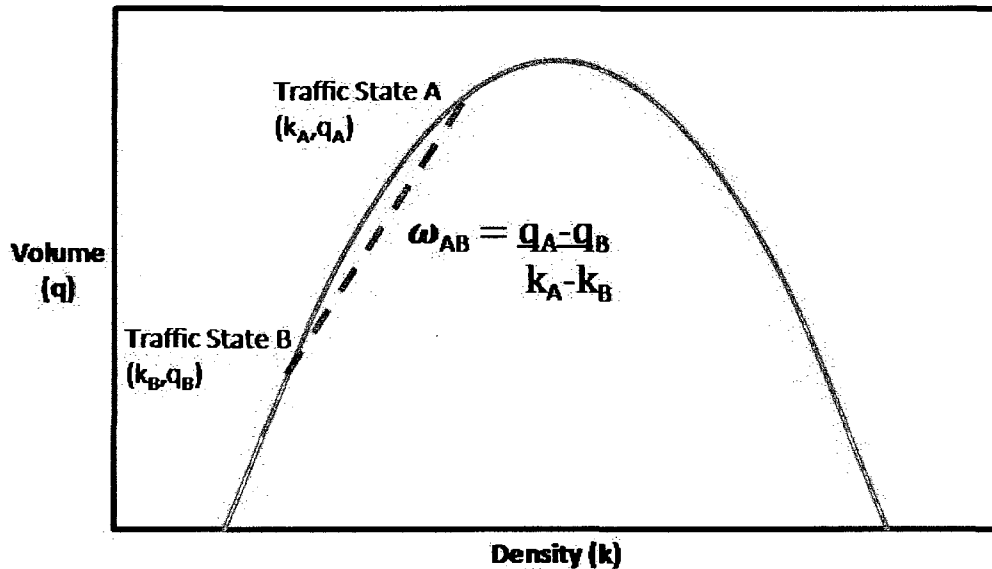


Figure 2.5: Calculating Shock Wave Speed

### 2.3 Real-Time Crash Analysis

To investigate the impact of traffic flow on crash likelihood, it is worthwhile to examine traffic conditions during the short time immediately before a crash occurs. Hall et al. (1986) concluded that real-time traffic analysis is advantageous in identifying patterns that exist on a roadway that may not be visible when using scatter diagrams of traffic data. They also found that the real time traffic analysis can identify transition points between congested and uncongested flow, which may not be visible in scatter diagrams.

Since real-time data has become readily available and easily accessed, numerous researchers in recent years have attributed analysis of real-time traffic flow on a freeway as an important tool for predicting crash likelihood. Oh et al. (2001) investigated the factors that contributed to traffic accidents in real-time using probability density functions distinguishing typical and disruptive traffic conditions, and concluded that the reduction in speed variation is crucial to reduce accident likelihood. Lee et al. (2002) investigated real-time crash precursors of variability on speed and traffic density on a stretch of freeway to predict potential for crashes using a log linear model, which accounted for exposures. The results of this paper indicate that these crash precursors are significant with controls for geometry, weather and time of day. Lee et al. (2003) expands the previous study by re-evaluating the model and suggesting methods to determine the crash precursors objectively and to test and compare this modified model with the previous model. After comparing these models, it was noted that the variables could be determined experimentally and less subjective judgment is required for determining categories of crash precursors. Another finding from this study was that crashes were more likely to occur when there was a significant difference in speed between a downstream and an upstream detector, indicating that the formation and/or dissipation of traffic queue is affecting crash risk.

Golob et al. (2004) presents a strong relationship between traffic flow conditions and likelihood of crashes. In this study, the mean volume and median speed, as well as the temporal variations in volume and speed determined 30 minutes prior to a crash occurrence had a strong association with the type of crash. The researchers in this study believe that identifying the type of crash is instrumental in enhancing safety on the roadway.

Abdel-Aty et al. (2004) developed a crash likelihood prediction model using real time traffic flow data and tested the crash identification percent. The first finding of the study was that 5 to 10 minute occupancy upstream of the crash site and the 5-minute coefficient of static variation in speed downstream of the crash site had the greatest impact on crashes. Using these factors, and with a threshold value of 1.0 for the log-odds ratio, 69% of the crash identification was achieved. From this conclusion, it can also be said that real time traffic data can indeed predict crashes. In a similar study, Songchitruksa and Balke (2006) determined that the same variables of 5-minute average occupancy and coefficient of variation in speed are good indicators of freeway crashes. The nested and nonnested multinomial logit models provided in this paper demonstrated how the variables mentioned detected the probability of an incident in the next 15-minutes using the real time data. Also, by comparing crash and non-crash data, there was a low false alarm rate. This paper also demonstrated factors other than traffic flow variables can determine the incident type using the same logit model. These factors included, visibility, lighting and time of day.

Pande and Abdel Aty (2005) expanded on a previous study to show the log of coefficient of temporal variation in speed, standard deviation of volume, and average occupancy expressed as percentage are significant in determining potential occurrence of a crash. Using these findings, another case-controlled logistic regression model was adapted to proactively determine whether or not a crash will occur, and using the data once again, the model was able to predict if a crash was going to occur in the upcoming 15 to 20 minute period. The authors also mention they have used a general model, and to use on a specific freeway, location, geometry, day, day of week would have to be used to calibrate the model to the particular section of freeway. Expanding on that study, Abdel Aty and Pemmanaboina (2006) modified the previous model to

include a rain index variable, and determined along with the rain index, the 5 minute average occupancy, the standard deviation of the volume downstream and 5 minute coefficient of variation in speed 5-10 minutes prior to the crash had significant affects on the crash occurrence and that it is possible to predict the likelihood of a crash prior to occurring.

A more empirical approach was studied by Hourdos et al. (2006). This study used individual vehicle speeds and headways from video cameras and tested the relationship between real time traffic conditions and likelihood of a crash by using only certain sections of the freeway with crash prone conditions, by first developing a model specific for the crash prone area. The authors also stress the importance of testing the models that are developed to test for accuracy. The crash model yielded a 58% success rate in predicting crashes, with only a 6.8% false detection rate. Qi et al. (2007) also presented an empirical analysis of real time traffic data to develop an accident frequency model using time series and cross sectional measures and the results indicated traffic flow characteristics, weather, and geometry were statistically significant with traffic accidents. A study by Son et al. (2009) used real-time individual vehicle and crash data similar to Hourdos et al. (2006) to determine shorter headway is more likely to contribute to crashes.

As mentioned in the previous section, the theory of shock waves was originally derived by Richards (1956) and Lighthill and Whitham (1957). Since then, researchers have used different methods to estimate shock wave speeds. Messer et al. (1976) used combined equations of the kinematic wave model and Greenshields' macroscopic traffic flow to estimate the speeds of shock waves formed after an incident occurs and a lane-blocking ensues. More recently, Hurdle and Son (2000) used density contour maps containing spatial and temporal propagation of



traffic regimes with similar densities to estimate the shock wave speeds. Expanding on the previous paper, Hurdle and Son (2001) used three examples to demonstrate that shock waves, arrival and departure curves for modeling freeway congestion curves are indeed compatible. Another method of shock wave estimation by Windover and Cassidy (2001) compared cumulative counts composed from vehicle counts. The previous two papers measured shock waves at fixed locations in the freeways studied; however Lu and Skabardonis (2007) determined shock waves based on individual vehicle trajectories under congested conditions. Although these papers discuss methods to determine shock waves, none of them has related the speed or type of shock wave to the likelihood of freeway crashes.

## 2.4 Evaluation of Literature

In recent years, many studies have been conducted to predict real-time crash risk using real-time measures of speed, volume and/or density for stretches of highways. These studies work better in predicting crashes than the studies that used average traffic data such as the annual average daily traffic volumes (AADT). The other advantage of using real-time data is that high crash risk can be detected in advance and crash occurrence can be potentially prevented before the crash actually occurs. This is valuable because it should significantly reduce the number of crashes once real time models can be implemented in traffic management systems. At the very least, traffic management centres can be prepared for incidents that may occur using real-time predictor models, leading to better response times when an incident occurs, thus decreasing wait times due to lane closures or blockages that may occur. Another important finding that has been noted in a majority of these studies that variations in speeds between loop detector stations is a strong indicator of crash occurrence, and the recommendations from these studies express the need for studying the effects of growth or dissipation of queue (shock waves) since

methods such as standard deviations some time period cannot show proper growth and dissipation effects.

Although shock wave speeds have been studied and methods to determine speed of shock wave are being established, there seems to be no link between this and crash likelihood methods. With the readily available short-term aggregated loop detector data, the choice of using this data as opposed to vehicle trajectories, as in the previous studies, needs to be investigated.

### 3 DATA

#### 3.1 Traffic Data

The data for this thesis were collected through loop detector stations located on a section of the Gardiner Expressway in Toronto, Ontario, Canada. The Gardiner Expressway is an urban freeway, frequently used by local commuters going to and from downtown Toronto. The studied section of the freeway analyzed has three lanes in each direction and is a fairly straight stretch of road. The westbound section is especially important because of the Jameson Ave. on ramp, which is closed from 3 pm to 6 pm in an attempt to alleviate congestion of the mainline traffic. An off-ramp is located upstream of the on-ramp, where significantly higher number of crashes occurs than other sections of the freeway (mainline station 80). The eastbound lanes have an on-ramp and two off-ramps on the studied section. The schematic drawing of this section of freeway is shown in Figure 3.1. Also shown in the figure are the distances between each of the loop detectors, in metres. The closest upstream station to the crash is assumed to be the crash location.

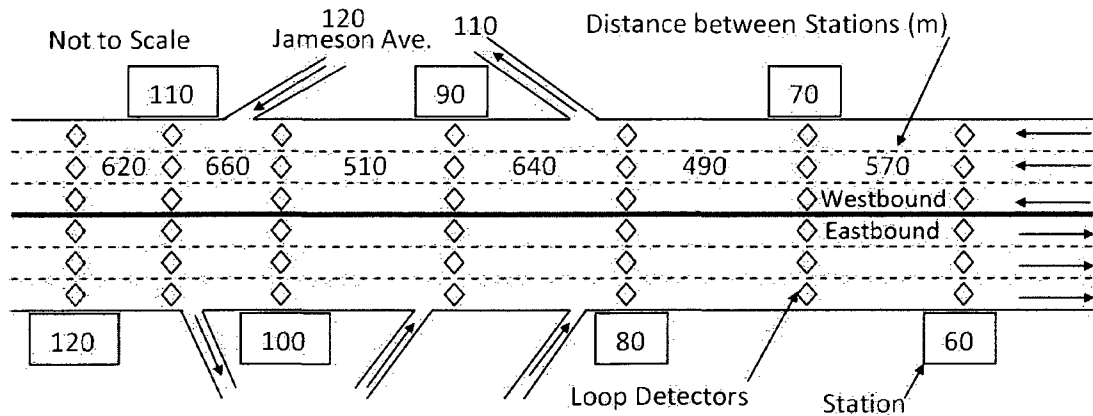


Figure 3.1: Detector Location on the Gardiner Expressway

The loop detectors monitor and record the 20-second volume, occupancy and speed data in each lane. The sections of interest were mainline stations 60, 70, 80, 90, 100, 110 and 120 for both eastbound and westbound lanes and ramp loop detector stations 110 and 120 in the westbound direction. For the ramp loop detector stations, only the one-lane 20-second volume was available. A total of 114 crashes occurred in the westbound lanes and 56 crashes occurred in the eastbound lanes for the 13-month period from January 1<sup>st</sup>, 1998 to January 31<sup>st</sup>, 1999. A sample of the raw data obtained at the loop detector station 60 is shown in Table 3-1.

Table 3-1: Sample Raw Data

TIME	SPEED (km/hr)			VOLUME (veh/hr)			OCCUPANCY (%)		
	median	middle	shoulder	median	middle	shoulder	median	middle	shoulder
18:00:03	37	41	54	2340	1800	2340	35	27	25
18:00:23	41	52	60	1800	1800	2160	25	22	22
18:00:43	44	51	59	1980	1980	1620	26	24	17
18:01:03	47	45	56	2160	1980	1620	27	29	19
18:01:23	49	52	56	2160	1800	1980	26	27	23
18:01:43	36	47	56	2340	2160	1800	38	29	19
18:02:03	29	49	56	1980	1980	2160	38	24	24
18:02:23	39	44	54	1980	1800	2340	29	27	25
18:02:43	43	49	58	1980	1980	1800	26	26	21

### 3.2 Incident Logs

Data for crashes were obtained through incident logs at the City of Toronto’s traffic management centre. Every incident which blocks one or more lanes of the freeway is logged and all of the following information is recorded: a unique ID (for cases that a crash occurred, this was the crash ID number), date (year, month, day, day of week), station (closest upstream station), the reported time and the weather condition. The time of crash occurrence was estimated based on the speed profiles using the time and speed values in each of the cases, and was determined to be the time when the speed abruptly drops. Figure 3.2 shows an example of the estimated time of crash at the detector station immediately upstream of the crash location.

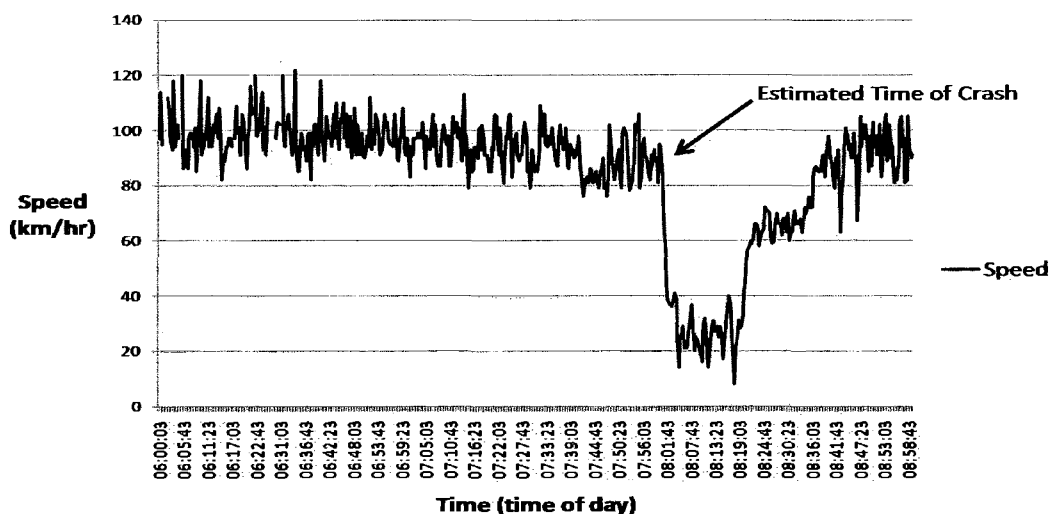


Figure 3.2: Speed Profile – Station 60

In traffic research, it is common that traffic flow conditions are distinctly different in the three time periods of the day – morning peak, afternoon peak and an off peak groups. This is the approach used for the eastbound traffic using a morning peak of 6 am to 9 am, an off peak period of 9 am to 3 pm and 8 pm to 11 pm, and an afternoon peak period from 3 pm to 8 pm. Due to the closure of the Jameson Ave. ramp, the afternoon peak period for the westbound lanes is further broken into two categories, afternoon peak with the ramp closed (from 3 pm to 6 pm) and afternoon peak with the ramp open (6 pm to 8 pm). The morning peak period runs the same as the eastbound lanes from 6 am to 9 am and the off peak period goes from 9 am to 3 pm and 8 pm to 11 pm (no crashes were recorded from 11 pm to 7 am in either direction).

### 3.3 Weather Data

Weather data for the freeway were also obtained. Hourly weather data, provided by Environment Canada, is labeled as either normal or adverse (rain, snow) condition each hour. Although different adverse weather conditions lead to different driver reactions, all of them were grouped due to lack of adverse weather data. In the 13-month period, 86.8% of the time

was considered to be normal weather conditions, and 13.2% of the time was considered to be adverse weather conditions.

### 3.4 Exposure

To account for the effect of exposure on crash frequency, exposure needs to be estimated. In traffic safety research, exposure is typically measured as the number of vehicles multiplied by the length of the road section.

The total number of vehicles\*kilometres for the 13-month period in each road section was calculated using daily traffic volume data obtained from loop detectors, AADT was multiplied by the length of the road section(i.e. distance between two successive loop detectors). This was multiplied by the number of weekdays in the 13-month period since this study only considers weekdays. The total exposures for road sections of each geometric type (straight, merging and diverging) are summarized in Table 3-2.

Table 3-2: Exposure for Each Road Section

Lane	Detector ID	Lanes	Road Type	AADT (veh/hr)	AADT (veh/day)	Distance (m)	Total veh*km	Total veh*km/13-month	Total veh*km/13-month	
WESTBOUND	dw0060dwg	3	straight	4,116	98,784	570	56,307	15,934,847	77,165,832	
	dw0070dwg	3	straight	4,104	98,495	490	48,263	13,658,312		
	dw0090dwg	3	straight	3,827	91,847	510	46,842	13,256,289		
	dw0110dwg	3	straight	4,209	101,014	620	62,629	17,723,943		
	dw0120dwg	3	straight	4,178	100,275	590	59,162	16,742,878		
	<b>TOTAL STRAIGHT</b>				<b>20,434</b>	<b>490,415</b>	<b>2,780</b>	<b>1,363,354</b>		<b>385,829,158</b>
	dw0100dwg	3	merging	3,612	86,681	660	57,209	16,190,205		16,190,205
	dw0080dwg	3	diverging	3,975	95,400	640	61,056	17,278,848		17,278,848
EASTBOUND	dw0060deg	3	straight	4,011	96,264	790	76,049	21,521,742	67,341,279	
	dw0070deg	3	straight	4,101	98,428	570	56,104	15,877,371		
	dw0080deg	3	straight	3,991	95,780	490	46,932	13,281,855		
	dw0120deg	3	straight	3,953	94,880	620	58,826	16,647,699		
	<b>TOTAL STRAIGHT</b>				<b>16,056</b>	<b>385,352</b>	<b>2,470</b>	<b>951,820</b>		<b>269,365,117</b>
	dw0090deg	3	merging	3,976	95,434	640	61,078	17,285,034		28,997,979
	dw0100deg	3	merging	3,514	84,331	500	42,166	11,932,891		
	<b>TOTAL MERGING</b>				<b>7,490</b>	<b>179,766</b>	<b>1,140</b>	<b>204,933</b>		
dw0110deg	3	diverging	3,949	94,765	670	63,492	17,968,377	17,968,377		

## 4 PROCEDURE

### 4.1 Classification of Shock waves

There are various ways of classifying shock waves based on the movement of shock wave between the two traffic states (A and B). This thesis classifies the shock waves based on three criteria. The first criterion is the direction of shock wave movement. If shock wave is moving in the same direction as the traffic flow (indicated by the positive slope of shock wave in the volume-density curve), it is classified as a forward moving shock wave. If shock wave is moving in the opposite direction of traffic flow (indicated by a negative slope of shock wave in the volume-density curve), it is classified as a backward moving shock wave.

The second criterion is the growth/dissipation of congestion. If the queue is growing over time (indicated by increasing density), the shock wave is forming. If the queue is dissipating over time (indicated by decreasing density), the shock wave is recovering.

The third criterion is the traffic state for each point. Some shock waves occur in the same traffic state (congested or uncongested) and some shock waves move between two traffic states (moving from congested to uncongested or vice versa). Using these three criteria, the following eight types of shock waves can be classified:

Type 1-1: Forward forming shock wave in uncongested region;

Type 1-2: Forward forming shock wave moving from uncongested to congested region;

Type 2-1: Forward recovery shock wave in uncongested region;

Type 2-2: Forward recovery shock wave moving from congested to uncongested region;

Type 3-1: Backward forming shock wave in the congested region;

Type 3-2: Backward forming shock wave moving from uncongested to congested region;



Type 4-1: Backward recovery shock wave in the congested region;

Type 4-2: Backward recovery shock wave moving from congested to uncongested region.

Each type of shock wave is shown graphically in Figure 4.1.

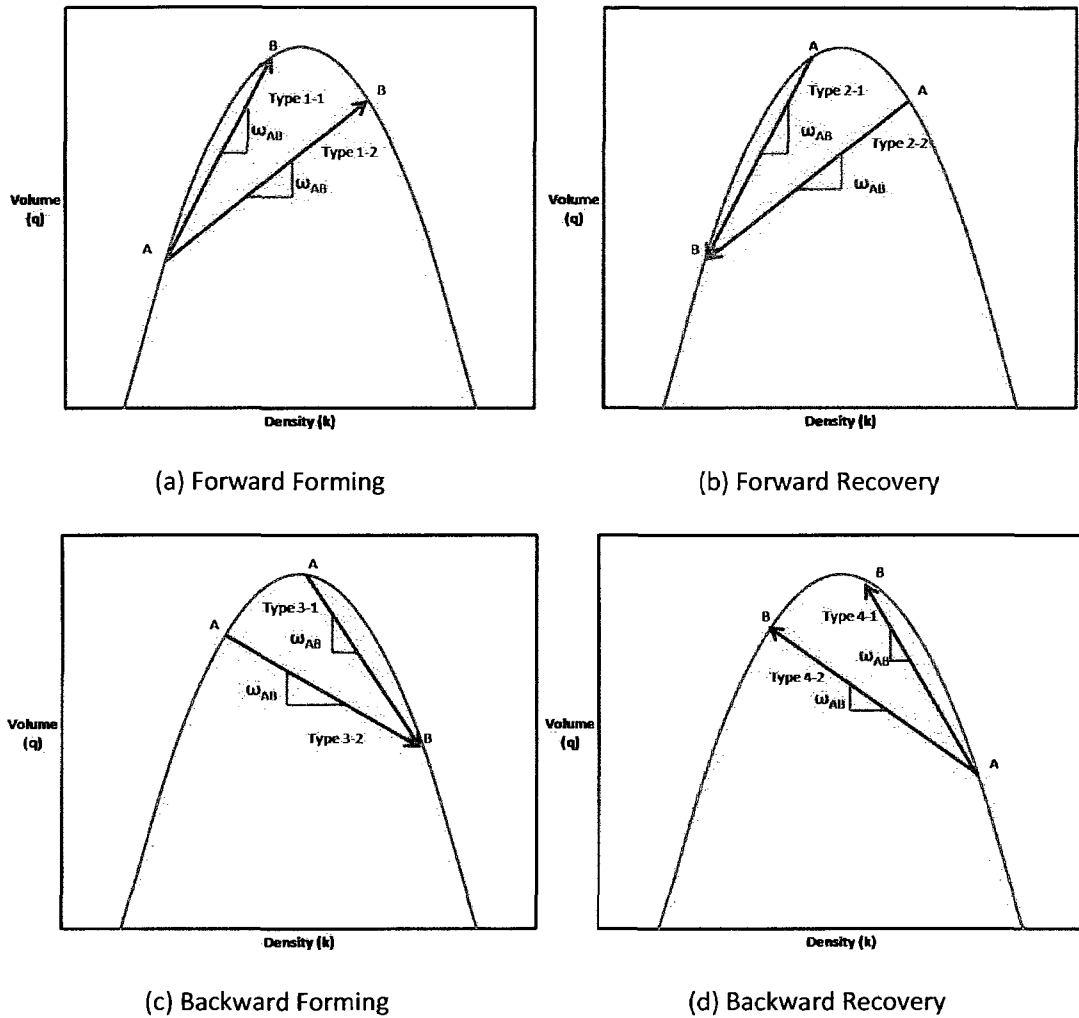


Figure 4.1: Shock wave Types

## 4.2 Critical Values and Trends

Prior to analyzing data, it was required to determine the critical density and capacity values on the freeway to identify the congested and uncongested states. To determine these values, 1-minute lane average volumes and densities were plotted on a graph to observe the general

volume-density relationship. This was done separately for different time periods of the day (morning peak, off peak, and afternoon peak periods) to observe the differences in traffic patterns. It was observed from these graphs that a critical density is approximately 30 veh/km and the roadway has a capacity of approximately 2300 veh/hour/lane.

Clear differences among the time periods were observed from the graphs. In the westbound lanes, the traffic flow conditions are split into four distinct time periods, morning peak, off peak, afternoon peak with the ramp closed and afternoon peak with the ramp open. In the morning peak period, more points are concentrated in the uncongested zone with fewer points in the congested zone. In the off peak period, points are more evenly scattered in both the uncongested zone and congested zone. In both of the afternoon peak periods, with and without ramp closure, a majority of points are scattered in the congested zone. However, the points are clustered around the critical density and capacity of the roadway when the ramp is closed, whereas more points are scattered in the congested region with the ramp open, likely due to the severe congestion when the ramp opens. The graphs are shown in Figure 4.2.

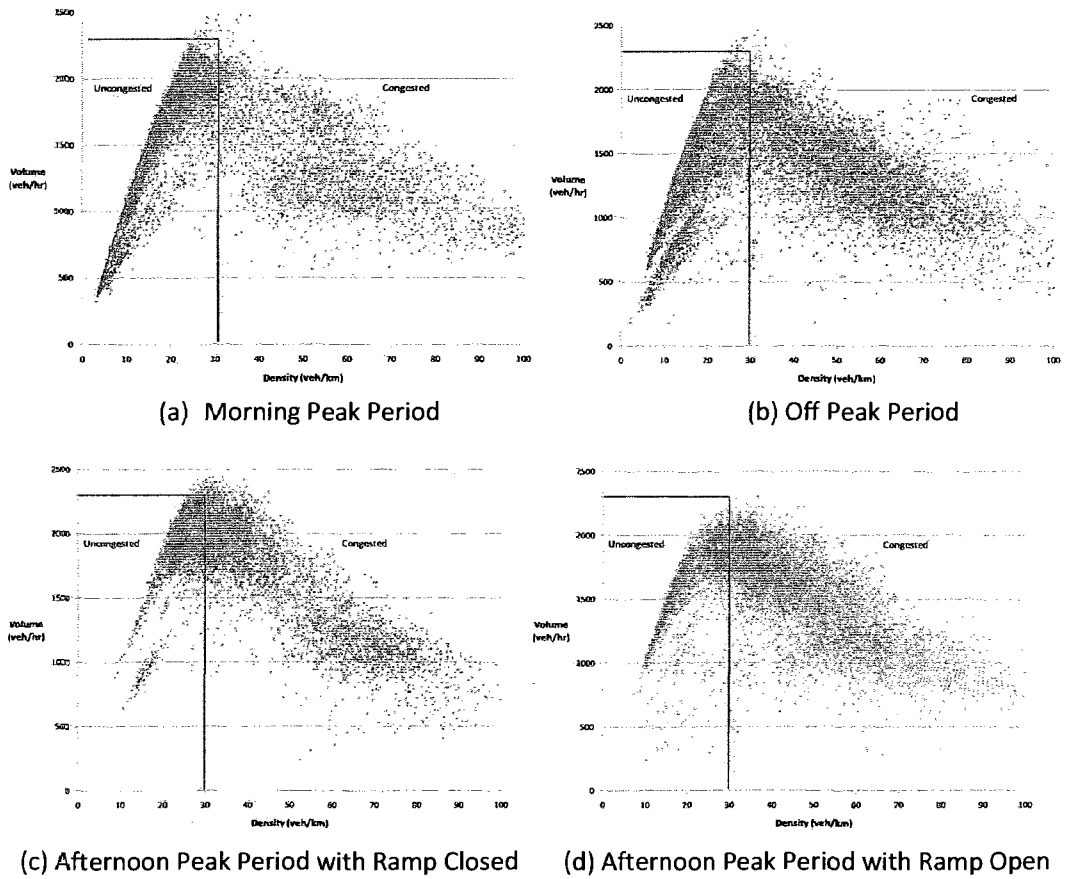
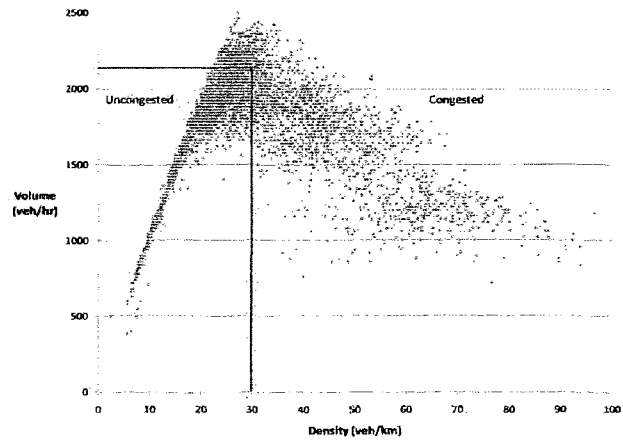
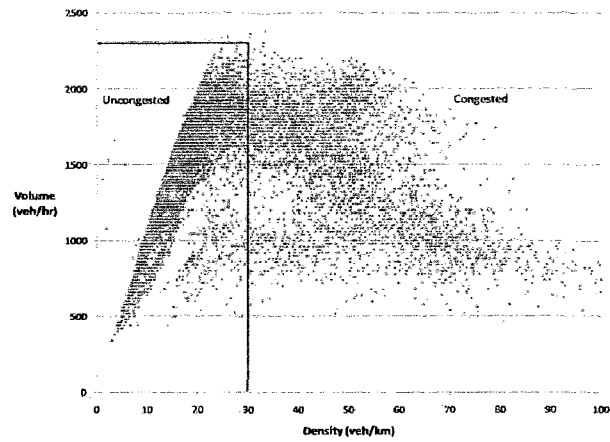


Figure 4.2: Volume-Density Graphs for Westbound Traffic

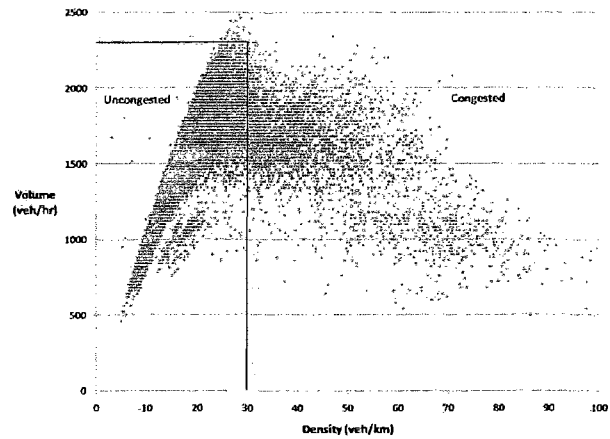
For the Eastbound traffic, only the typical three time periods were used, morning peak period, off peak and afternoon peak period because there was no ramp closure. A strong linear trend can be observed in the morning peak period in the uncongested zone, with a small cluster of points in the congested zone. A similar trend was observed in the uncongested zone, but more points are scattered in the congested zone during the off-peak period. Finally, similar volume-density pattern was observed during the afternoon peak period. The volume-density graphs for the eastbound traffic are shown in Figure 4.3. Overall, the volume-density patterns are not distinctly different in the eastbound traffic unlike the westbound traffic.



(a) Morning Peak Period



(b) Off Peak Period



(c) Afternoon Peak Period

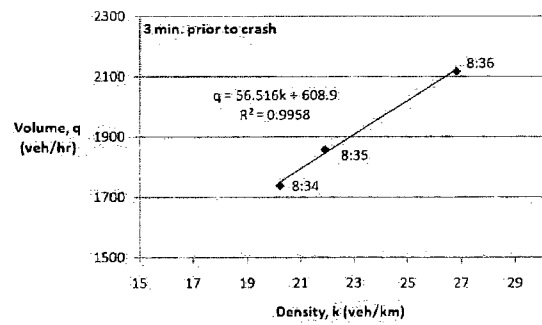
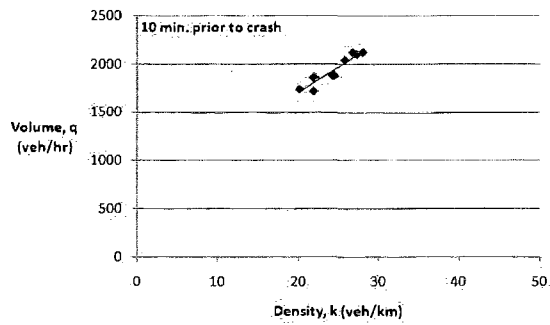
Figure 4.3 : Volume-Density Graphs for Eastbound Traffic

### 4.3 Determining Shock wave

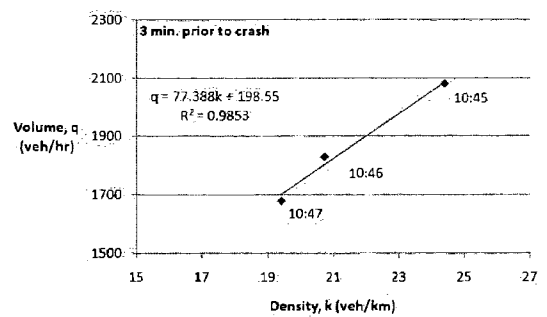
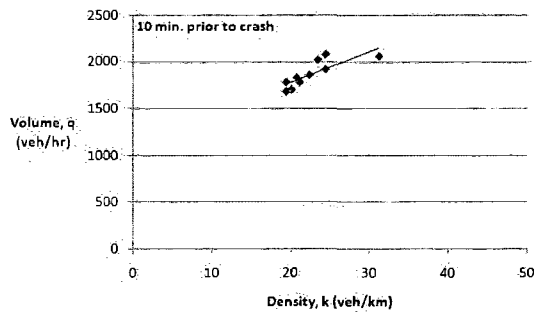
Once the critical density and capacity were determined from the volume-density graphs, a volume-density curve was plotted for a ten-minute period (arbitrarily chosen) prior to the time of crash for each crash case. Although the original data were recorded in 20-second intervals, one-minute cumulative average data were used to account for possible random fluctuation of values in the data. In each crash case, the presence of shock wave was checked. If shock wave was present, the type and speed of the shock wave were measured. Shock waves were measured in two ways. In the first method, if the points showed a linear trend, simple linear regression was used to calculate the shock wave speed as shown in Figure 4.4 three or four minutes prior to crash time. This method was used mainly for crashes that stayed in the same zone (uncongested or congested) since they showed linear trends. The second method was to take an average of the cluster of points in different parts of the last ten minutes then measuring the slope of the line between the dots representing the average of the cluster of points. Figure 4.5 (a) shows no real trend of the points, but by taking the average of the clusters of the first two points and the average of the last six points and joining the two average points, good shock wave estimation is produced as shown in Figure 4.5 (b). This method was not used often, but was typically used for cases that switched from uncongested zone to congested zone or vice versa.

In the westbound lanes, there were a total of 114 crashes, with 62 cases (54%) showing a shock wave occurrence in the last 10-minutes, and 75 cases (66%) in the last 3-10 minutes (called "short term") prior to the crash time. Of the 56 crashes in the eastbound lanes, 28 cases (50%) showed a shock wave in the last 10-minutes, whereas 36 cases (64%) showed a shock wave in

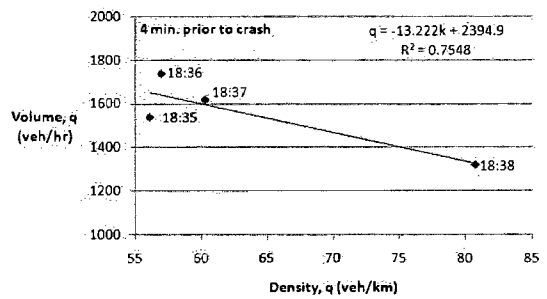
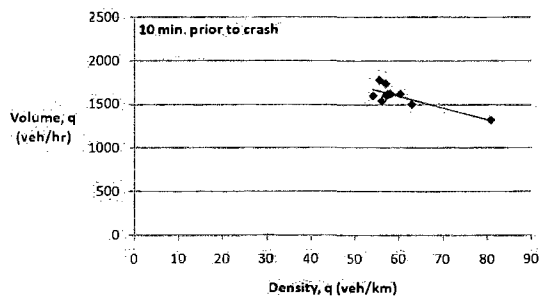
the short term prior to the crash time. Figure 4.4 shows examples of different shock wave types observed in the last ten minutes and the short term prior to the crash time.



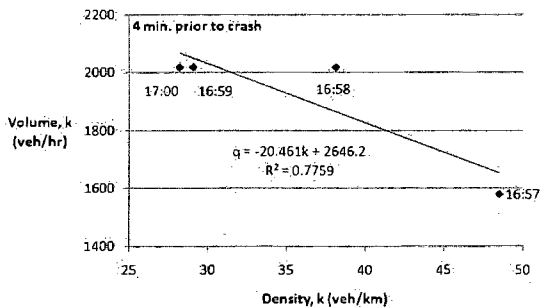
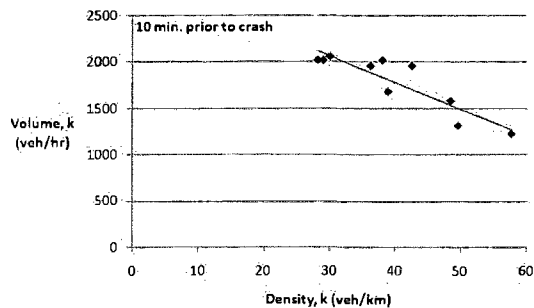
(a) Forward Forming Shock wave (Morning Peak – WBL)



(b) Forward Recovery Shock wave (Off-Peak – EBL)



(c) Backward Forming Shock wave (Afternoon Peak – Entrance Ramp Open – WBL)



(d) Backward Recovery Shock wave (Afternoon Peak – Entrance Ramp Closed – WBL)

Figure 4.4: Shock wave Types

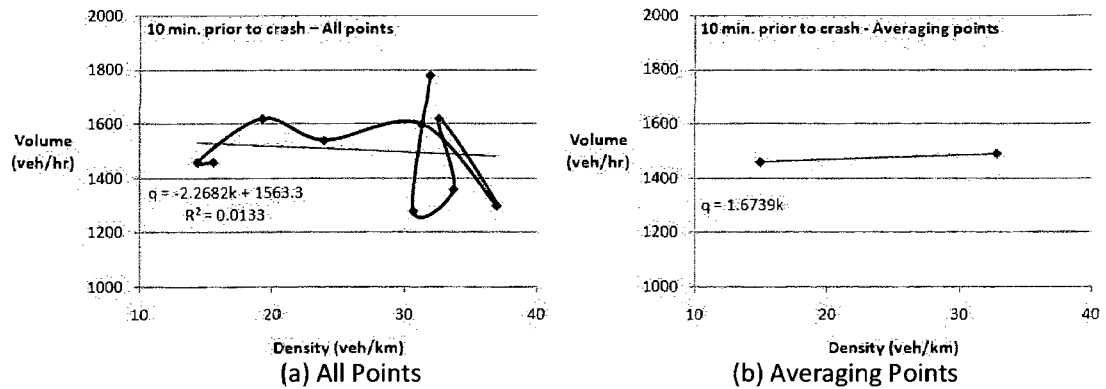


Figure 4.5: Averaging Points

In Figure 4.4, it can be observed that the shock wave type observed in the short term is not always consistent with the shock wave type observed in the last ten minutes. Since the short term changes immediately before crash occurrence are more likely to affect crash occurrence, the shock wave type observed in the short term may be more important than the one observed in the longer term.

#### 4.4 Effect of Ramps on Mainline Traffic

Ramp traffic can directly or indirectly influence the flow of traffic on the freeway. In particular, mainline detector station 80 immediately upstream of the off ramp accounted for 56% of the total crashes in the study period. Thus, it is possible that the ramp traffic may have contributed to high number of crashes. For this reason, traffic volume on ramp prior to crash time were collected from loop detectors and compared graphically with the mainline traffic volume.

#### 4.5 Statistical Analysis Techniques

Some statistical analysis techniques are used to investigate the effect of shock wave on crash likelihood. The theoretical background of the two statistical models – logistic regression model and log-linear model – is explained in this section.



#### 4.5.1 Logistic Regression Model

Logistic regression model is ideal for the analysis, using the variables are dichotomous (e.g. crash or non-crash). The model eliminates the lower and upper bound that limits linear regression (Allison, 1999). The logistic regression model is described in the following equation:

$$\ln \frac{P(Y=i)}{1-P(Y=i)} = \alpha + \beta_1 x_{i1} + \beta_2 x_{i2} + \dots + \beta_k x_{ik} \quad (3)$$

Where,

$P(Y = i)$  = the probability of occurrence of a crash ( $i = 1$  for crash and  $i = 0$  for non-crash);

$\alpha$  = a constant;

$\beta_k$  = a coefficient for the explanatory variable;

$x_{ik}$  = explanatory variable.

The left side of the equation denotes the probability of crash ( $Y=1$ ) to the probability of non-crash ( $Y=0$ ). Another name for this ratio is the odds of crash to non-crash. This is a popular model because the coefficients are simple to understand, and the model can be generalized to allow for multiple unordered categories for the dependent variable (Allison, 1999).

#### 4.5.2 Log Linear Model

The log linear model is ideal for identifying impacts of factors on crash frequency accounting for the exposure. The exposure takes into account the frequency of events that may cause crashes so that the likelihood of crash occurrence (or crash rate) can be estimated more logically. For example, since most days are in normal weather conditions more crashes tend to occur in normal weather conditions. However, this does not necessarily mean normal weather conditions are more likely to contribute to crashes than adverse weather conditions. Similarly, there are more sections of road that are straight than there are curved road sections and more crashes tend to occur on straight road sections. However, this does not necessarily mean that crashes are more likely to occur on the straight road section.

For instance, the log-linear model including two categorical variables A and B is described in the following equation:

$$\ln(F_{ij}) = \mu + \lambda_i^A + \lambda_j^B + \lambda_{ij}^{AB} + \beta_{\text{exp}} * \ln(\text{exp}) \quad (4)$$

Where,

- $\mu$  = intercept;
- $F_{ij}$  = expected frequency for variable A with category i and variable B with category j;
- $\lambda_i^A, \lambda_j^B$  = main effect variables on frequency (i.e. parameters that change according to the category of variable A or B);
- $\lambda_{ij}^{AB}$  = interaction effect of variables A and B on frequency (i.e. parameter that change according to the categories of variable A and B);
- $\beta_{\text{exp}}$  = coefficient of the exposure measure;
- exp = exposure.

The relationship between expected frequency and explanatory variables is assumed to be non-linear to avoid potential negative frequency values (Jovanis and Chang, 1986). From this, it is assumed that these variables are not correlated. The above equation is a saturated model because it includes all the one-way and two-way effects. The model becomes unsaturated if some of the effects are zero. If the  $\lambda_{ij}^{AB}$  term is removed, the model becomes an independence model, meaning that A has no effect on B or vice versa (Jeansonne, 2002).

Crashes distribution does not follow a normal distribution since the plot of the number of road sections against the number of crashes does not have a symmetrical distribution. It is expected that there will be a high number of crashes at only a few road sections, meaning a higher peak sooner in the graph and a long tail with few crashes. For this reason, the distributions of expected frequency are commonly assumed to follow Poisson distribution or negative binomial distribution. First the Poisson distribution is defined as follows (Jovanis and Chang, 1986):

$$P_i(k) = \frac{(e^{-\lambda_i t}) * (\lambda_i t)^k}{k!} \quad (5)$$

Where,

- $P_i(k)$  = probability that frequency of event is ( $k=0, 1, 2, 3, \dots$ );
- $\lambda_i$  = expected value of event frequency for  $i$ th interval;
- $t$  = number of intervals.

The Poisson distribution assumes that the mean and the standard deviation of the distribution are equal. However, if the variance is far greater than the mean (called “over-dispersion”), this assumption of Poisson is no longer valid. Hauer (2001) explains that when over dispersion may occur, meaning the differences between accident counts and model predictions are larger than what would be consistent with the assumption of Poisson distributed accident counts. For this reason, negative binomial regression is preferred by researchers to represent the distribution of accidents. The negative binomial distribution using the overdispersion parameter is as follows (Hauer, 2001):

$$P(Y_i = y_i) = \frac{\Gamma(y_i + \phi)}{\Gamma(\phi) y_i!} \left(\frac{\phi}{\eta_i + \phi}\right)^{\eta_i} \left(\frac{\eta_i}{\eta_i + \phi}\right)^{y_i} \quad (6)$$

Where,

- $Y_i$  = random variable of accident counts on entity  $i$ ;
- $y_i$  = specific accident count on entity  $j$ ;
- $\phi$  = overdispersion parameter;
- $\eta_i$  = expected number of events.

The Pearson Chi-Squared statistic is commonly used to test for goodness-of-fit of the log-linear model and independence of two variables. This test is useful to determine if an observed frequency distribution differs from a theoretical distribution and also assesses whether or not two variables are independent of each other (Agresti, 2002). The statistic is calculated using the following equation:

$$\chi = \sum_j \frac{(n_j - \mu_j)^2}{\mu_j} \quad (7)$$

Where,

$\chi$  = chi-squared statistic;  
 $n_j$  = observed frequency;  
 $\mu_j$  = expected frequency.

The expected frequencies estimated by log-linear analysis can also be used to estimate the relative probability of a certain case compared to a base case. The relative probability is computed by dividing the expected frequency of the case by the expected frequency of the base case. This ratio is defined as the “odds ratio”. The odds ratio is calculated using the following equation:

$$\begin{aligned} \ln\left(\frac{F_{ij}}{F_{1j}}\right) &= \ln(F_{ij}) - \ln(F_{1j}) \\ \ln\left(\frac{F_{ij}}{F_{1j}}\right) &= (\theta + \lambda_{x(i)} + \lambda_{y(j)} + \lambda_{xy(ij)}) - (\theta + \lambda_{x(1)} + \lambda_{y(j)} + \lambda_{xy(1j)}) \\ \ln\left(\frac{F_{ij}}{F_{1j}}\right) &= (\lambda_{x(i)} - \lambda_{x(1)}) + (\lambda_{xy(ij)} - \lambda_{xy(1j)}) \\ \frac{F_{ij}}{F_{1j}} &= e^{(\lambda_{x(i)} - \lambda_{x(1)})} * e^{(\lambda_{xy(ij)} - \lambda_{xy(1j)})} \end{aligned} \quad (8)$$

Where,

$F_{ij}$  = expected frequency of case;  
 $F_{1j}$  = expected frequency of base case;  
 $\theta$  = constant;  
 $\lambda_{x(i)}, \lambda_{y(i)}$  = coefficients for variables X and Y;  
 $\lambda_{xy(ij)}, \lambda_{xy(1j)}$  = coefficient for interaction of variables X and Y;  
 $\lambda_{x(1)}$  = coefficient for base case.

The odds ratio greater than 1 implies that the case is more likely to occur than the base case.

The odds ratio less than 1 implies that the case is less likely to occur than the base case.

## 5 RESULTS AND ANALYSIS

### 5.1 Shock waves

In the previous chapter, the procedure for measuring a shock wave was presented. Using a critical density of 30 veh/km and a capacity of 2300 veh/hr, shock wave speed and type described in chapter 2 were determined. The results show 28 cases (50%) and 36 cases (64%) in the 10-minute and short term period, respectively, for the 56 crashes in the eastbound lanes and 62 cases (54%) and 75 cases (66%) in the 10-minute and short term period for the 114 westbound lane crashes. Table 5-1 shows the breakdown of crashes by type for each time period. Majority of the non-classified crash cases occurred in the congested period after the ramp opens in the afternoon, due to the large fluctuation of the data points during that time period.

Table 5-1: Shock waves Sorted by Shock wave Type (Crash Cases)  
(a) Westbound Lanes

TYPE	AM Peak		Off Peak		PM Peak Ramp Closed		PM Peak Ramp Open	
	10 minute	short term	10 minute	short term	10 minute	short term	10 minute	short term
<b>1-1</b>	<b>13</b>	<b>7</b>	<b>14</b>	<b>13</b>	<b>9</b>	<b>7</b>	<b>2</b>	<b>1</b>
<b>1-2</b>	<b>0</b>	<b>0</b>	<b>1</b>	<b>1</b>	<b>1</b>	<b>1</b>	<b>2</b>	<b>4</b>
<b>2-1</b>	<b>3</b>	<b>9</b>	<b>1</b>	<b>3</b>	<b>0</b>	<b>4</b>	<b>0</b>	<b>1</b>
<b>2-2</b>	<b>0</b>	<b>0</b>	<b>0</b>	<b>1</b>	<b>1</b>	<b>0</b>	<b>1</b>	<b>1</b>
<b>3-1</b>	<b>0</b>	<b>0</b>	<b>0</b>	<b>0</b>	<b>2</b>	<b>1</b>	<b>4</b>	<b>4</b>
<b>3-2</b>	<b>0</b>	<b>0</b>	<b>0</b>	<b>0</b>	<b>0</b>	<b>0</b>	<b>0</b>	<b>0</b>
<b>4-1</b>	<b>0</b>	<b>0</b>	<b>0</b>	<b>2</b>	<b>1</b>	<b>1</b>	<b>0</b>	<b>6</b>
<b>4-2</b>	<b>0</b>	<b>0</b>	<b>0</b>	<b>0</b>	<b>5</b>	<b>6</b>	<b>2</b>	<b>2</b>
<b>NO TYPE</b>	<b>10</b>	<b>10</b>	<b>13</b>	<b>9</b>	<b>9</b>	<b>8</b>	<b>20</b>	<b>12</b>
<b>TOTAL</b>	<b>26</b>	<b>26</b>	<b>29</b>	<b>29</b>	<b>28</b>	<b>28</b>	<b>31</b>	<b>31</b>

(b) Eastbound Lanes

TYPE	AM Peak		Off Peak		PM Peak	
	10 minute	short term	10 minute	short term	10 minute	short term
1-1	1	1	4	5	5	5
1-2	0	0	0	0	1	1
2-1	3	3	5	7	6	6
2-2	0	1	0	1	1	1
3-1	0	0	0	0	0	1
3-2	1	1	0	0	0	0
4-1	0	0	1	1	0	0
4-2	0	2	0	0	0	0
NO TYPE	5	2	11	7	12	11
<b>TOTAL</b>	<b>10</b>	<b>10</b>	<b>21</b>	<b>21</b>	<b>25</b>	<b>25</b>

It was found that the total number of cases where shock waves were observed generally greater for the short term than the 10-minute time period. This may be because a shock wave can occur within a time frame shorter than 10 minutes typically three to five minutes prior to the crash. If there was no trend, meaning the last few points were not in the same direction, but the density and volume were either increasing or decreasing, the whole 10-minute period was used.

It was also found that a majority of the crashes occurred as shock waves move forward (i.e. in the same direction of traffic flow). The higher number of backward moving shock waves was observed in the afternoon peak period on the westbound lanes, both with the ramp closed and with the ramp open. This is reasonable because a queue forms more frequently during these congested time periods. During the three-hour period when the Jameson Ave. ramp is closed, the road conditions are near capacity and after the ramp opens, there is a large influx of vehicles that enter the freeway.

An average value was taken to determine typical speeds by shock wave type. Table 5-2 shows the average shock wave values by type.

Table 5-2: Average Shock wave Speed by Type (Crash Cases)  
(a) Westbound Lanes

TYPE	AM Peak		Off Peak		PM Peak Ramp Closed		PM Peak Ramp Open	
	10 minute	short term	10 minute	short term	10 minute	short term	10 minute	short term
1-1	60.62	59.86	69.82	70.76	47.92	53.42	34.95	64.44
1-2	—	—	2.27	1.67	7.80	19.80	28.22	30.92
2-1	49.22	54.84	70.71	60.35	—	55.14	—	33.19
2-2	—	—	—	42.15	15.10	—	11.96	24.23
3-1	—	—	—	—	-21.72	-25.90	-18.30	-19.21
3-2	—	—	—	—	—	—	—	—
4-1	—	—	—	-28.11	-29.00	-54.49	—	-20.05
4-2	—	—	—	—	-19.94	-16.07	-14.40	-14.40

(b) Eastbound Lanes

TYPE	AM Peak		Off Peak		PM Peak	
	10 minute	short term	10 minute	short term	10 minute	short term
1-1	62.02	62.02	66.41	58.50	52.74	51.64
1-2	—	—	—	—	7.11	7.11
2-1	51.46	61.11	59.86	57.51	65.18	67.62
2-2	—	26.17	—	16.55	1.05	1.05
3-1	—	—	—	—	—	-38.16
3-2	-21.06	-21.06	—	—	—	—
4-1	—	—	-21.34	-21.34	—	—
4-2	—	-21.92	—	—	—	—

For most cases, the average shock wave speeds are relatively similar. The only notable exception is in the afternoon peak period for the ramp closed in the westbound lanes, which has a value of -54.49 km/hr. As expected, the type 1-1 and type 2-1 shock waves produce the highest shock wave values, because queue is either forming or dissipating solely in the uncongested zone and a typical volume-density graph for shock waves shows a better trend in the uncongested regime. Also, in real time, it is difficult to quantify speed, volume and occupancy values in the congested regime due to the fluctuation of points.

To identify the effect of shock wave on crash likelihood, shock waves were also estimated for the normal traffic conditions when a crash did not occur. Shock waves were observed in the same manner as the crash cases using the loop detector data obtained during normal traffic conditions. These data are called “non-crash” data. The non-crash data were obtained from the same detector station and at the same time period and weather conditions as the crash data but on different weekdays when a crash did not occur. The purpose of this data extraction is to control for the confounding effects of road geometry and weather on crash likelihood.

For the non-crash data, 43 cases (77%) in the 10-minute period and 46 cases (82%) in the short term period of the eastbound lanes showed a type of shock wave, whereas for the westbound lanes, 75 cases (66%) in the 10-minute period and 84 cases (74%) in the short term period showed some type of shock wave. In every period, the non-crash data had more cases of shock waves occurring than in the crash cases. It was found that the shock wave speeds differ for each time period for crash and non-crash cases. The results are broken up again by shock wave type as shown in Table 5-3.

Table 5-3: Shock waves by Shock wave Type (Non-Crash Cases)  
(a) Westbound Lanes

TYPE	AM Peak		Off Peak		PM Peak Ramp Closed		PM Peak Ramp Open	
	10 minute	short term	10 minute	short term	10 minute	short term	10 minute	short term
1-1	12	11	12	13	9	11	2	3
1-2	0	0	0	0	2	3	3	3
2-1	9	11	5	4	4	3	0	2
2-2	0	0	0	0	1	0	3	1
3-1	0	0	1	2	2	3	3	4
3-2	0	0	0	0	0	1	2	0
4-1	0	1	0	1	1	1	3	5
4-2	0	0	0	0	0	0	1	1
NO TYPE	5	3	11	9	9	6	14	12
TOTAL	26	26	29	29	28	28	31	31



## (b) Eastbound Lanes

TYPE	AM Peak		Off Peak		PM Peak	
	10 minute	short term	10 minute	short term	10 minute	short term
<b>1-1</b>	2	2	6	6	6	7
<b>1-2</b>	2	1	0	0	0	1
<b>2-1</b>	2	2	5	5	14	13
<b>2-2</b>	0	1	0	0	0	0
<b>3-1</b>	0	0	0	0	0	0
<b>3-2</b>	1	1	1	1	1	1
<b>4-1</b>	2	2	0	0	0	0
<b>4-2</b>	0	0	1	2	0	1
<b>NO TYPE</b>	1	1	8	7	4	2
<b>TOTAL</b>	<b>10</b>	<b>10</b>	<b>21</b>	<b>21</b>	<b>25</b>	<b>25</b>

Table 5-3 shows that a dominant type of shock wave is forward moving shock waves, similar to the crash cases. The total number of crashes with an observed visible shock wave is again greater for the short term data than the 10-minute data, for the same reason as the crash cases. In addition, more backward moving shock waves were observed in the afternoon peak periods of the westbound lanes. Overall, both the crash and non-crash cases show similar totals of crashes of shock waves by type. The average shock wave values shown in Table 5-4 and have the same patterns occurring between crash and non-crash cases as well, with the higher shock wave speeds for the forward moving shock waves, and lower speeds for the backward moving shock waves.

Table 5-4: Average Shock wave Speed by Type (Non-Crash Cases)

(a) Westbound Lanes

TYPE	AM Peak		Off Peak		PM Peak Ramp Closed		PM Peak Ramp Open	
	10 minute	short term	10 minute	short term	10 minute	short term	10 minute	short term
1-1	69.01	70.47	77.74	77.87	59.80	63.21	82.36	67.59
1-2	—	—	—	—	35.83	34.87	34.34	36.37
2-1	58.96	67.21	69.78	70.73	53.68	51.65	—	59.96
2-2	—	—	—	—	32.69	—	21.99	41.92
3-1	—	—	-11.75	-12.31	-20.36	-19.89	-16.05	-33.12
3-2	—	—	—	—	—	-2.50	-8.17	—
4-1	—	-43.08	—	-24.93	-37.04	-37.04	-18.22	-13.13
4-2	—	—	—	—	—	—	-14.41	-16.36

(b) Eastbound Lanes

TYPE	AM Peak		Off Peak		PM Peak	
	10 minute	short term	10 minute	short term	10 minute	short term
1-1	51.04	64.80	76.66	77.58	73.04	63.77
1-2	30.51	48.76	—	—	—	35.99
2-1	47.24	41.94	82.46	82.73	69.19	68.05
2-2	—	20.05	—	—	—	—
3-1	—	—	—	—	—	—
3-2	-15.30	-17.43	-4.40	-4.40	-24.07	-24.07
4-1	-19.85	-22.85	—	—	—	—
4-2	—	—	-24.27	-17.73	—	-43.87

For a detailed comparison of the results presented, the average shock wave values have been computed. The average forward moving shock wave is 60.63 km/hr and 60.27 km/hr in the eastbound and westbound directions respectively. These values are well below the average of 100 km/hr from the findings of Hurdle and Son (2001). The reason this occurs is Hurdle and Son (2001) measured forward moving shock waves based on free flow speed, and this study measures it at free flow speed, as well as times when the flow is near congestion. As it is shown in the previous charts as well as through analysis of the volume-density curve, the shock wave speed is significantly lower near the capacity, and when the shock wave is in transition between the congested and uncongested phases (type 1-2 and type 2-2). The average backward moving shock waves of 22.72 km/hr and 22.53 km/hr in the eastbound and westbound direction

respectively are comparable to the values of 18.34 km/hr from Lu and Skabardonis (2007) and 25 km/hr from Hurdle and Son (2001).

The distributions of shock wave speed are shown in Figure 5.1 for the eastbound and westbound lanes. Conventionally, backward moving shock waves are negative based on the formula of a shock wave (the volume and density will carry different signs) but for analysis, an absolute value is used. It is interesting to note that in both cases, a higher shock wave speed is observed for the non-crash cases. This is against the expectation that a faster moving shock wave has a higher influence on crash risk.

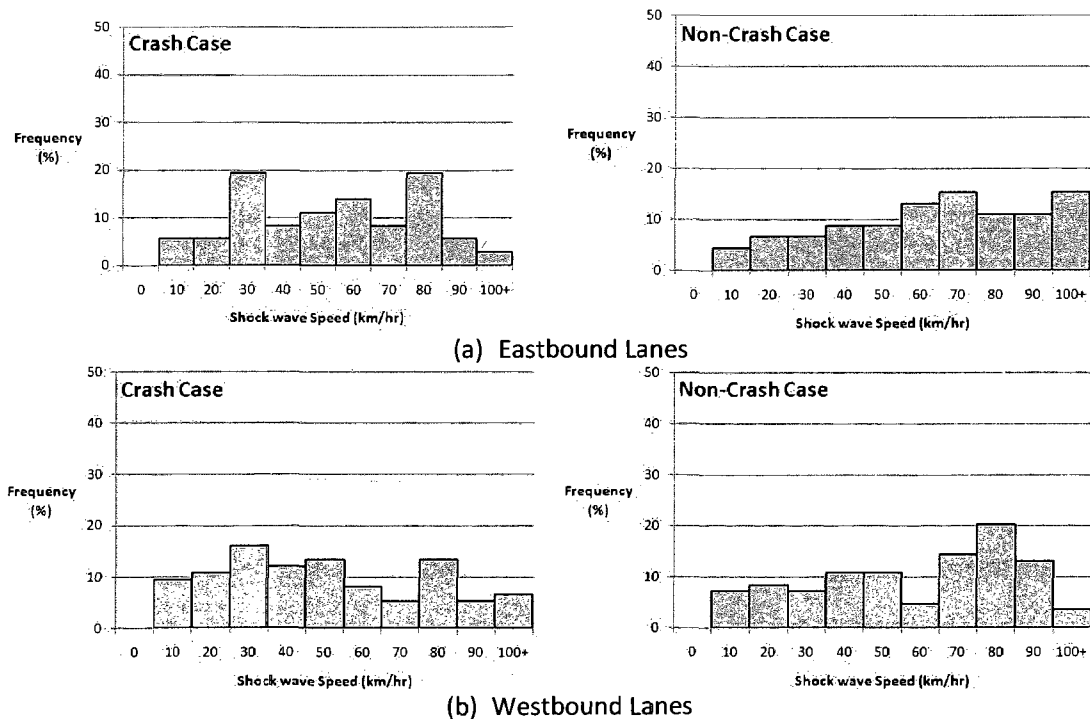


Figure 5.1: Frequency of Crashes

Thus, the distributions of shock wave speed were compared separately for the two different directions of movement – a forward moving wave or a backward moving wave. Figure 5.2 (a) shows the forward moving shock wave distribution for the eastbound lanes and Figure 5.2 (b)

shows the distribution for the westbound lanes. It is clear in both cases that a faster moving forward shockwave has a positive effect on crash risk. This conclusion is conceivable because when vehicles progress faster in uncongested zone or vehicles depart from a congested region faster, the vehicles approaching the congested area are less likely to slow down and consequently crash likelihood decreases. This is consistent with findings from Abdel-Aty et al. (2007), where faster removal of congestion prevents growth of queue, but also reduces crash risk.

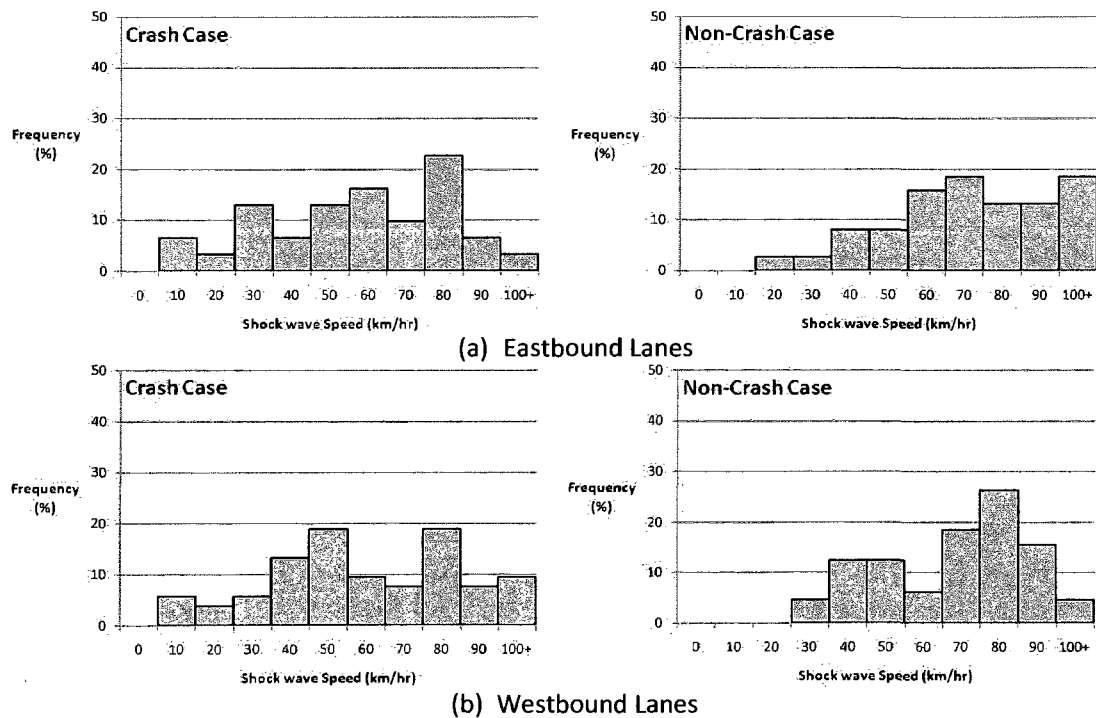


Figure 5.2: Frequency of Crashes – Forward Shock waves

In the case of backward moving shock waves, as shown in Figure 5.3, there seems to be a higher frequency of cases with faster moving shock waves in the crash cases than in the non-crash cases. This would lead to the conclusion that a faster moving backward shock wave has higher crash likelihood. A higher crash risk with a faster moving backward shock wave is plausible, given that when a queue grows faster, it is difficult for vehicles entering queue to react quicker

and adjust speeds to avoid a crash. Unfortunately, there are a limited number of cases available for proper comparison.

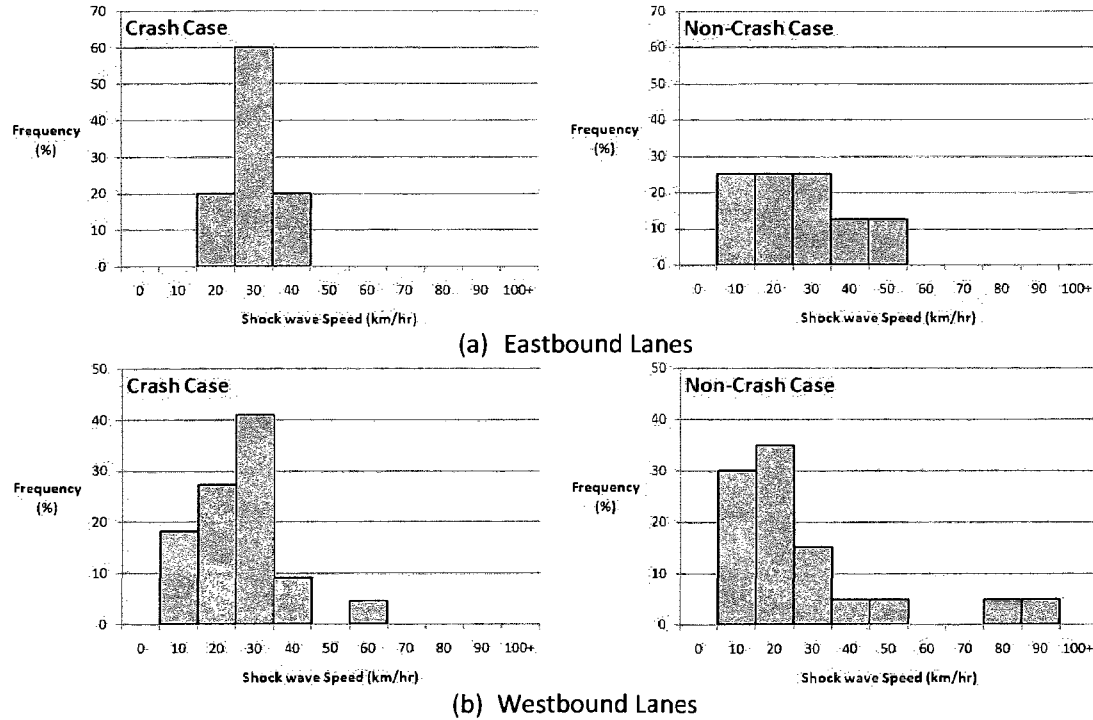


Figure 5.3: Frequency of Crashes— Backward Shock waves

Detailed results of shock wave type and speed for both crash and non-crash cases in both the 10-minute and short term periods can be found in Appendix A.

## 5.2 Effect of Ramps on Mainline Traffic

Data was available for the on and off ramps in the westbound lanes for 60 of the 114 crash cases. This data was used to analyze what effect the ramps have on traffic conditions prior to a crash. Figure 5.4 graphically compares the mainline stations (60, 70, 80, 90, and 100) to the off ramp (110) and the on ramp (120) for one crash case. In this particular case, the crash occurs at 18:32:03, the time when the volume is decreasing, but both the on and off ramps do not seem to be effected by the crash occurrence. Similar phenomena were observed in all other cases.

This may be because the detector stations on ramps are distant from the area influenced by mainline traffic. Due to this limitation, no further analysis was conducted in the scope of this thesis.

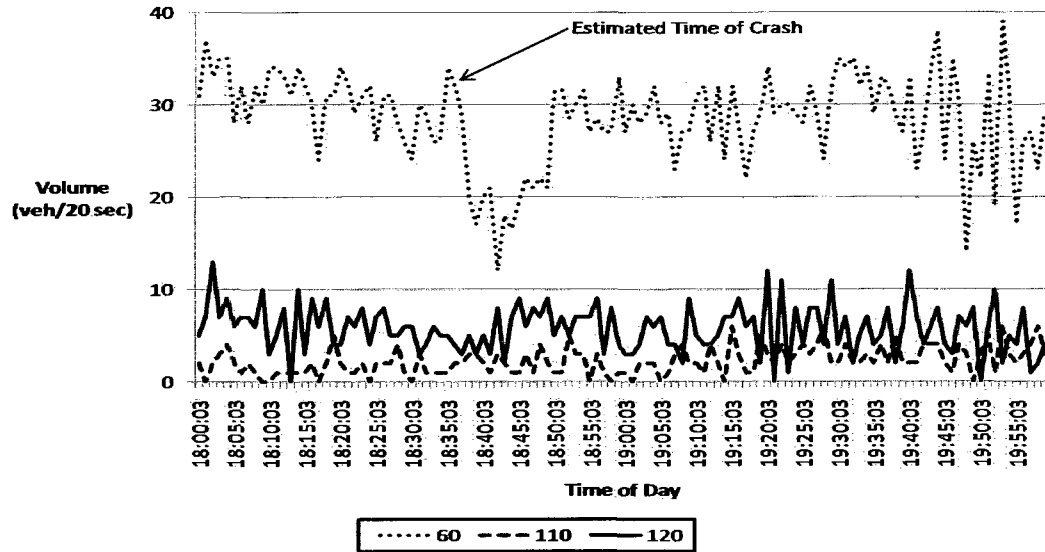


Figure 5.4: Comparison of Ramp and Mainline Traffic Volumes

### 5.3 Ideal Time Period

Throughout the course of this thesis, both the 10-minute and short term periods have been evaluated thus far. However, given that there are more cases available with the short term data and the traffic conditions during the short term period prior to the crash time has a greater impact on the traffic; the short term data were used for future analysis.

### 5.4 Logistic Regression Model

The results in section 5.1 show that the distributions of frequency were different between crash and non-crash cases. To determine the statistical significance of these results, a logistic regression is used to develop a model based on shock wave speed. In this particular model, the time of day, geometry and weather conditions are controlled for since these variables are the same for both crash and non-crash cases. Thus, the pure effect of the shock wave type and

speed on crash likelihood can be tested. Following the results in section 5.1, the cases have been split up by the type of shock wave.

Several variables such as shock wave speed, forming and recovery waves, and change in zone and no change in zone waves were considered to develop a model for different directions of shock wave movement. Among the variables, only shock wave speed was found to be the significant factor. For the case of forward moving shock waves in the eastbound lanes, the logistic regression model was estimated as follows:

$$\ln \frac{P(Y=i)}{1-P(Y=i)} = 1.2820 - 0.0247 * \text{ShockSpeed} \quad (9)$$

where ShockSpeed is the actual shock wave speed in km/hr. For the westbound lanes, logistic regression model was estimated as follows:

$$\ln \frac{P(Y=i)}{1-P(Y=i)} = 1.0319 - 0.0205 * \text{ShockSpeed} \quad (10)$$

The shock wave speed was statistically significant at a 95% confidence interval with the p-values of 0.0267 and 0.0332, respectively. The negative coefficients indicate that a slower moving forward shock wave will increase the odds of a crash. This means that faster progression of vehicles will not only help alleviate congestion, but also reduce the chance of a crash occurrence.

Similar analysis was performed for the backward moving shock waves. In both cases (eastbound and westbound), no significant variables was found. Although there was no significant variable, it is worth to note that the sign of the coefficient was positive, which indicate a faster moving backward shock wave would increase the odds of a crash. To confirm this assumption, more cases of backward moving shock waves are needed.

## 5.5 Log linear Model

As mentioned in the previous chapter, the log linear model is ideal for the crash analysis because it can account for the exposure. Annual average traffic volume (AADT), road geometry (straight, merge or diverge) and weather conditions (normal or adverse) were considered as exposure. Weather conditions were labeled as normal for days with good weather and were marked adverse for the rest of the days, whether it was heavy rain, drizzle, snow, sleet, or any other condition. They were labeled in this manner to avoid multiple factors for weather and to avoid zero values when calculating exposure. For the log linear model, only the crash cases are used for the two directions of traffic flow (eastbound and westbound). Four categorical variables including geometry, weather, shock wave type (forward or backward) and shock wave speed (low or high) were considered in the development of this model. An interaction term between shock wave type and shock wave speed is also considered in this analysis.

The shock wave speeds were categorized as low or high speed based on the median value for the non-crash cases in their respective direction of travel (64.96 km/hr for eastbound lanes and 60.29 km/hr for westbound lanes). The exposure is the only continuous variable in the model. The values for calculated exposure rate in veh-km are given in Table 3-2, with the values for normal and adverse weather conditions being 86.8% and 13.2%, respectively. To calculate the exposure for the given road section and given weather condition, total AADT for each road section type is multiplied by the percentage of time for normal or adverse weather conditions. Negative binomial regression model was developed to avoid the assumption from the Poisson regression (mean = standard deviation).



In the eastbound lanes, the weather, type and speed were found to have statistical significance at 95% using a total of 36 cases, based on the Poisson analysis and the model for this is:

$$\ln(F_{ij}) = -8.95 + \lambda_{\text{WEATHER}} + \lambda_{\text{SHOCKTYPE}} + \lambda_{\text{SHOCKSPEED}} + 0.434 * \ln(\text{exp}) \quad (11)$$

Where,

$F_{ij}$	= expected frequency of crash;
$\lambda_{\text{WEATHER}}$	= coefficient for weather (normal or adverse);
$\lambda_{\text{SHOCKTYPE}}$	= coefficient for shock wave type (forward or backward);
$\lambda_{\text{SHOCKSPEED}}$	= coefficient for shock wave speed (low or high);
exp	= continuous value of exposure.

The interaction term between shock wave type and shock wave speed is not significant in the eastbound lanes. The coefficients for each variable are given in Table 5-5. Negative binomial regression did not yield any significant results. However, Poisson regression may be used in this instance because the overdispersion does not exist, indicated by the Pearson Chi-Square divided by degrees of freedom (1.0312) being close to one. When comparing the values from the base values, positive coefficients for normal weather conditions, forward moving shock waves and low shock wave speed indicates that these factors contribute to higher crash likelihood than the adverse weather conditions, backward moving shock waves, and high shock wave speed, respectively. The positive effect of normal weather conditions is likely due to the fact drivers can be less cautious when driving in normal weather conditions. Also, due to better visibility, it can be speculated that drivers are more inclined to use excessive speeds, and attempt passing maneuvers.

Table 5-5: Results of Log Linear Model - Eastbound Lanes

Condition		Value	p-value
$\lambda_{\text{WEATHER}}$	Normal	1.26	0.0174
	Adverse	0	—
$\lambda_{\text{SHOCKTYPE}}$	Forward	1.82	0.0002
	Backward	0	—
$\lambda_{\text{SHOCKSPEED}}$	Low	0.82	0.0233
	High	0	—

In the westbound lanes, negative binomial regression is used with a total of 75 cases and all of the factors tested are statistically significant at 95%. The formula for the westbound lanes is:

$$\ln(F_{ij}) = -7.38 + \lambda_{\text{GEOMETRY}} + \lambda_{\text{WEATHER}} + \lambda_{\text{SHOCKTYPE}} + \lambda_{\text{SHOCKSPEED}} + \lambda_{\text{TS}} + 0.434 * \ln(\text{exp}) \quad (12)$$

Where,

- $F_{ij}$  = expected frequency of crash;
- $\lambda_{\text{GEOMETRY}}$  = coefficient for geometric condition (straight, merging or diverging);
- $\lambda_{\text{WEATHER}}$  = coefficient for weather (normal or adverse);
- $\lambda_{\text{SHOCKTYPE}}$  = coefficient for shock wave type (forward or backward);
- $\lambda_{\text{SHOCKSPEED}}$  = coefficient for shock wave speed (low or high);
- $\lambda_{\text{TYPESPEED}}$  = coefficient for interaction between shock wave type and shock wave speed;
- exp = continuous value of exposure.

Since the Pearson Chi-Square parameter divided by the degrees of freedom is close to one (1.68), the overdispersion does not exist in this model. The model also considers an interaction term between the shock wave type and shock wave speed. This term will be used later for log-odds ratio calculations. Comparing the coefficients shown in Table 5-6 in a similar fashion to the eastbound lanes, normal weather conditions, forward moving shock waves and lower speed shock waves are all positive contributors to crash risk. The comparison of coefficients for three geometry variables shows that the diverging section has the highest crash risk (indicated by the highest coefficient value), followed by the merging sections and then by the straight sections of

roads. This result can be attributed to more difficulty with reducing speed to exit from mainline freeway in the diverging road sections compared to other road section types.

Table 5-6: Results of Log Linear Model - Westbound Lanes

Condition		Value	p-value
$\lambda_{\text{GEOMETRY}}$	Straight	-1.52	< 0.0001
	Merging	-1.41	< 0.0001
	Diverging	0	—
$\lambda_{\text{WEATHER}}$	Normal	0.84	0.0041
	Adverse	0	—
$\lambda_{\text{SHOCKTYPE}}$	Forward	1.76	0.0004
	Backward	0	—
$\lambda_{\text{SHOCKSPEED}}$	Low	1.71	0.0008
	High	0	—
$\lambda_{\text{TYPESPEED}}$	Forward and Low	-1.36	0.0197
	Forward and High	0	—
	Backward and Low	0	—
	Backward and High	0	—

Using the formulas above, the expected frequency of crashes for each case can be calculated. For example, the expected frequency for the westbound lanes for the 13-month period on straight section, under normal weather conditions, in the case of a forward moving shock wave and a low shock wave speed is calculated as follows:

$$\ln(F_{ij}) = -7.38 + \lambda_{\text{GEOMETRY}} + \lambda_{\text{WEATHER}} + \lambda_{\text{SHOCKTYPE}} + \lambda_{\text{SHOCKSPEED}} + \lambda_{\text{TYPESPEED}} + \beta_{\text{exp}} * \ln(\text{exp})$$

$$\ln(F_{11}) = -7.38 + (-1.52) + 0.84 + 1.76 + 1.71 + (-1.36) + (0.434) * \ln(66,995,375)$$

$$\ln(F_{ij}) = 1.88$$

$$F_{ij} = e^{1.88}$$

$$F_{ij} = 6.55$$

The expected frequencies can be calculated in a similar manner for all cases, and compared with the observed frequencies to check for model fit. The results for the eastbound and westbound lanes are shown in Table 5-7. The observed and expected frequencies correspond well for the eastbound lanes; however there is more variance in the westbound lanes. The observed and expected frequencies are different because of the high number of zero cells in the westbound lanes.

Table 5-7: Observed and Expected Frequencies  
(a) Eastbound Lanes

WEATHER →		OBSERVED		EXPECTED	
		Normal	Adverse	Normal	Adverse
SHOCKTYPE	SHOCKSPEED				
Forward	Low	18	2	19.14	2.39
Forward	High	9	2	8.42	1.05
Backward	Low	5	0	3.09	0.39
Backward	High	0	0	1.36	0.17
TOTAL		32	4	32.01	4.00

(b) Westbound Lanes

WEATHER →			OBSERVED		EXPECTED	
			Normal	Adverse	Normal	Adverse
SHOCKTYPE	SHOCKSPEED	GEOMETRY				
Forward	Low	Straight	4	0	6.58	1.25
		Merging	3	1	3.73	0.71
		Diverging	16	6	15.68	2.98
Forward	High	Straight	8	0	4.61	0.88
		Merging	5	0	2.61	0.50
		Diverging	8	2	10.98	2.09
Backward	Low	Straight	7	0	4.41	0.84
		Merging	1	0	2.50	0.47
		Diverging	13	1	10.50	2.00
Backward	High	Straight	0	0	0.80	0.15
		Merging	0	0	0.45	0.09
		Diverging	0	0	1.90	0.36
TOTAL			65	10	64.75	12.32

As mentioned in the earlier, the exposure is essential to estimate the impact of factors on crash likelihood. The results of the log linear models with and without exposure measures were

compared. As shown in Table 5-7, there is noticeable difference between the two models. Although the positive effect of normal weather conditions remains unchanged, the coefficient has been increased in the model without exposure. In terms of road geometry, the coefficient for the straight sections is now higher than the coefficient for the merging sections (i.e. crash likelihood is higher on straight sections) although both coefficients are still lower than the coefficient for the diverging sections. This result is counter-intuitive since drivers usually have more difficulty with speed change and lane change on the merging section than the straight section, crash likelihood is more likely to be higher on the merging section. The differences stem from the fact that the model without exposure only considers the total number of crashes and neglects the difference in exposure. As shown in Table 3-2, the total vehicle-kilometres of travel for straight section is almost five times greater than the merging section (77 million veh\*km/13 months compared to 16 million veh\*km/13 months). This means that inherently higher crash frequency on the straight section than the merging section is expected due to the longer road section and higher traffic volume. Thus, the results from the model with exposure are considered more valid and realistic.

**Table 5-8: Exposure Comparison – Westbound Lanes**

<b>Condition</b>		<b>With Exposure</b>	<b>Without Exposure</b>
<b>Intercept</b>		<b>-7.38</b>	<b>-1.02</b>
<b>Geometry</b>	<b>Straight</b>	<b>-1.52</b>	<b>-0.87</b>
	<b>Merging</b>	<b>-1.41</b>	<b>-1.44</b>
	<b>Diverging</b>	<b>0</b>	<b>0</b>
<b>Weather</b>	<b>Normal</b>	<b>0.84</b>	<b>1.66</b>
	<b>Adverse</b>	<b>0</b>	<b>0</b>

Finally, odds ratios were computed to evaluate the effects of the interaction between shock wave type and speed on the crash frequency for the westbound lanes. The formula derived in

the previous chapter is used for calculations of the odds ratio. The backward moving shock wave is set as base case. A sample calculation is shown below for the forward moving shock wave at a low speed.

$$\frac{F_{ij}}{F_{1j}} = e^{(\lambda_{x(0)} - \lambda_{x(1)})} * e^{(\lambda_{xy(0i)} - \lambda_{xy(1j)})}$$

$$\frac{F_{00}}{F_{10}} = e^{(\lambda_{x(0)} - \lambda_{x(1)})} * e^{(\lambda_{xy(00)} - \lambda_{xy(10)})}$$

$$\frac{F_{00}}{F_{10}} = e^{(1.76-0)} * e^{[(-1.36)-0]}$$

$$\frac{F_{00}}{F_{10}} = 1.49$$

Table 5-9 compares the odds ratio. The odds ratio greater than 1 for the forward moving shock wave indicate that forward shock waves have a greater effect on crash risk than the backward moving shock wave cases at both high and low shock wave speeds. However, the relative impacts of forward moving shock wave to backward moving shock wave differ between high and low shock wave speeds (1.49 and 5.81, respectively).

Table 5-9: Log-odds Ratio - Westbound Lanes

		Shock wave Speed	
		Low (0)	High (1)
Shock wave Type	Forward (0)	1.49	5.81
	Backward (1)	1	1

## 6 CONCLUSIONS AND RECOMMENDATIONS

### 6.1 Conclusions

Overall, several conclusions can be drawn based on the analysis. First, a new insight was provided in determining shock wave speed. The presence of shock wave speed can be estimated in real time using real-time traffic flow data and the volume-density relationship. The estimated shock wave speeds were generally consistent with findings from other researchers. Second, shock waves occur during a short time period before a crash occurrence and their patterns are different in different time periods of the day. Using these important findings from this thesis, the movement of queue was found to have significant effects on crash risk.

Using the shock wave speeds for crash and non-crash data on the stretch of studied freeway, logistic regression models and log linear models were constructed to predict the likelihood of crashes. The results of the logistic regression models show that as the speed of a forward moving shock wave decreases crash likelihood increases. In contrast, the opposite trend was observed for the backward moving shock waves. As the speed of backward moving shock wave increases, crash likelihood also increases in spite of the statistical insignificance of the results due to the lack of data.

*The results of the log linear model show that normal weather conditions, forward moving shock waves and high shock wave speeds increase the crash likelihood in both the eastbound and westbound lanes. In the westbound lanes, it was also found that the road geometric conditions were significant, with diverging sections having the highest crash likelihood, followed by merging sections and straight sections. It is important to note that the inclusion of exposure in the model produces different results and represents the effect of each factor on crash frequency*

more intuitively. Lastly, there exists an interaction between shock wave speed and shock wave type on crash frequency. It was found based on the odds ratios that forward moving shock waves have greater effect on crash likelihood than backward moving shock waves at both high and low shock wave speed. This relative effect is more significant when shock wave speed is higher.

## 6.2 Recommendations

Several recommendations are made based on the current findings. The first and most important recommendation is to analyze the effect of backward moving shock waves on freeway crash likelihood using additional data. It is also recommended to investigate “spatial” (not only temporal) propagation of shock wave and its consequent effect on crash likelihood using the traffic flow data both upstream and downstream of the crash locations. In addition, the traffic data on ramps at the location closer to the mainline freeway can help capture the effect of ramp traffic volume on shock wave and crash likelihood. To evaluate the transferability of the findings, the same methodology can be applied to other sections of the studied freeway and other freeways. Along the same lines, another set of detector and crash data in a longer time period can be used for the same section of freeway to validate the models. Also, the effects of other exploratory variables such as the number of lanes (if they are different across the sections) can be examined. Also, the volume-density relationship can be altered based on the weather conditions to produce a different graph in adverse conditions. By doing this, the shock wave types may change, and may give slightly different results. Lastly, methodology to automatically measure shock wave speed and type based on real-time data needs to be investigated for real-time applications.



As far as the practical applications are concerned, the findings of this research can be applied to real time crash predictions and development of crash mitigation strategies, such as variable speed limits and driver warning messages.

## REFERENCES

- Abdel Aty, Mohamed A. and Pemmanaboina, Rajashekar. (2006). Calibrating a Real-Time Traffic Crash-Prediction Model Using Archived Weather and ITS Traffic Data. *IEEE Transactions on Intelligent Transportation Systems* , 7 (2), 167-174.
- Abdel Aty; M., Dilmore, J.; Hsia, L. (2006). Applying Variable Speed limits and the Potential for Crash Mitigation. *Transportation Research Record* , 1953, 21–30.
- Abdel-Aty, Mohamed; Nizam, Uddin; Pande, Anurag; Abdalla, M. Fathy; Hsia, Liang. (2004). Predicting Freeway Crashes from Loop Detector Data by Matched Case-Control Logistic Regression. *Transportation Research Record* , No. 1897, 88-95.
- Agresti, Alan. (2002). *Categorical Data Analysis Second Edition*. Hoboken, New Jersey: John Wiley & Sons, Inc.
- Allison, Paul D. (1999). *Logistic Regression Using the SAS System: Theory and Application*. Cary, NC: SAS Institute Inc.
- Cody, R. (2007). *Learning SAS by Example: A Programmer's Guide*. Cary, NC: SAS Institute Inc.
- Golob, Thomas F.; Recker, Wilfred W.; Alvarez, Veronica M. (2004). Freeway safety as a function of traffic flow. *Accident Analysis and Prevention* , 36, 933-946.
- Hall, Fred L.; Allen, Brian L.; Gunter, Margot A. (1986). Empirical Flow Analysis of Freeway Flow-Density Relationships. *Transportation Research A* , 20A, 197-210.
- Hauer, Ezra. (2001). Overdispersion in modelling accidents on road sections and in Empirical Bayes Estimation. *Accident Analysis and Prevention* , 33, 799-808.
- Hourdos, John N.; Garg, Vishnu; Michalopoulos, Panos G.; Davis, Gary A. (2006). Real-Time Detection of Crash-Prone Conditions at Freeway High-Crash Locations. *Transportation Research Record* , No. 1968, 83-91.
- Hurdle, V.F. and Son, Bongsoo. (2000). Road Test of a Freeway Model. *Transportation Research Part A* , 34, 537-564.
- Hurdle, V.F. and Son, Bongsoo. (2001). Shock Wave and Cumulative Arrival and Departure Models - Partners Without Conflict. *Transportation Research Record* , 1776, 159-166.
- Jeansonne, Angela. (2002, September 26). *Loglinear Models*. Retrieved June 2009, from Loglinear Models:  
<http://userwww.sfsu.edu/~efc/classes/biol710/loglinear/Log%20Linear%20Models.htm>
- Jovanis, Paul P. and Chang, Hsin-Li. (1986). Modeling the Relationship of Accidents to Miles Travelled. *Transportation Research Record* , 1068, 42-51.

- Lapin, Lawrence L. (1996). *Modern Engineering Statistics*. Belmont, CA: Wadsworth Publishing Company.
- Lee, Chris; Hellinga, Bruce; Saccomanno, Frank. (2003). Real-Time Crash Prediction Model for the Application to Crash Prevention in Freeway Traffic. *Transportation Research Record*, No. 1840, 67-77.
- Lee, Chris; Saccomanno, Frank; Hellinga, Bruce. (2002). Analysis of Crash Precursors on Instrumented Freeways. *Transportation Research Record*, No. 1784, 1-8.
- Lighthill, M. H. and G. B. Whitham, G. B. (1957). On Kinematic Waves II: A Theory of Traffic Flow on Long Crowded Roads. *Proceedings of the Royal Society*, 229 (Series A), 317-345.
- Lu, Xiao-Yun, and Skabardonis, Alexander. (2007). Freeway Traffic Shockwave Analysis: Exploring the NGSIM Trajectory Data. *Presented at the 86th Transportation Research Board Annual Meeting*. Washington, D.C.
- Messer, C. J.; Dudek, C. L.; Friebele, J. D. (1976). Method for Predicting Travel Time and Other Operational Measures in Real-Time During Freeway Incident Conditions. *Transportation Research Record*, 567, 1-16.
- Oh, Jun-Seok; Oh, Cheol; Ritchie, Stephen G.; Chang, Myungsoon. (2001). Real-Time Estimation of Accident Likelihood for Safety Enhancement. *Journal of Transportation Engineering*, 131 (5), 358-363.
- Pande, Anurag and Abdel-Aty, Mohamed. (2005). A Freeway Safety Strategy for Advanced Proactive Traffic Management. *Journal of Intelligent Transportation Systems*, 9 (3), 145-158.
- Qi, Yi; Smith, Brian L.; Guo, Jianhua. (2007). Freeway accident likelihood prediction using a panel data analysis approach. *Journal of Transportation Engineering*, 133 (3), 149-156.
- Richards, P. I. (1956). Shock Waves on the Highway. *Operations Research*, 4 (1), 42-51.
- Son, Hojun; Kweon, Young-Jun; Park, Byungkyu. (2009). Development of Crash Prediction Models with Individual Vehicle Data. *Presented at the 88th Transportation Research Board Annual Meeting*. Washington, D.C.
- Songchitruksa, Praprut and Balke, Kevin N. (2006). Assessing Weather, Environment, and Loop Data for Real-Time Freeway Incident Prediction. *Transportation Research Record*, No. 1959, 105-113.
- Windover, John R., and Cassidy Michael J. (2001). Some Observed Details of Freeway Traffic Evolution. *Transportation Research Part A*, 35, 881-894.

## **APPENDIX A**

**TABLE A-1: Shock wave Types for Crash Cases**

LANE	TIME PERIOD	CRASH ID	10 MINUTE		SHORT TERM	
			TYPE	SPEED	TYPE	SPEED
East	AM Peak	1185	2-1	51.18	2-1	51.18
East	AM Peak	1482	0		0	
East	AM Peak	2224	0		4-2	-25.62
East	AM Peak	3540	2-1	76.54	2-1	105.48
East	AM Peak	6278	3-2	-21.06	3-2	-21.06
East	AM Peak	6312	0		0	
East	AM Peak	7419	0		4-2	-18.21
East	AM Peak	8165	2-1	26.66	2-1	26.66
East	AM Peak	8386	0		2-2	26.17
East	AM Peak	9280	1-1	62.02	1-1	62.02
East	Off Peak	161	4-1	-21.34	4-1	-21.34
East	Off Peak	169	1-1	54.94	1-1	54.94
East	Off Peak	450	0		0	
East	Off Peak	547	2-1	87.15	2-1	87.15
East	Off Peak	1250	0		2-2	16.55
East	Off Peak	1254	2-1	60.52	2-1	77.39
East	Off Peak	1866	0		0	
East	Off Peak	1936	0		0	
East	Off Peak	3647	0		2-1	54.36
East	Off Peak	5969	1-1	79.65	1-1	79.65
East	Off Peak	6235	0		0	
East	Off Peak	6419	0		2-1	27.78
East	Off Peak	6928	2-1	49.44	2-1	49.44
East	Off Peak	7125	0		0	
East	Off Peak	7349	2-1	73.21	2-1	73.21
East	Off Peak	7430	0		0	
East	Off Peak	7523	1-1	38.27	1-1	26.78

East	Off Peak	7637	1-1	92.78	1-1	78.62
East	Off Peak	8675	0		1-1	52.49
East	Off Peak	9307	0		0	
East	Off Peak	9865	2-1	28.98	2-1	33.24
East	PM Peak	91	0		3-1	-38.16
East	PM Peak	143	0		0	
East	PM Peak	901	2-1	59.11	2-1	59.11
East	PM Peak	1285	0		0	
East	PM Peak	1813	0		0	
East	PM Peak	1978	0		0	
East	PM Peak	2019	1-2	7.11	1-2	7.11
East	PM Peak	3302	2-1	64.39	2-1	79.01
East	PM Peak	3801	2-1	65.57	2-1	65.57
East	PM Peak	5816	0		0	
East	PM Peak	6167	0		0	
East	PM Peak	6246	2-1	83.74	2-1	83.74
East	PM Peak	6293	2-2	1.05	2-2	1.05
East	PM Peak	6569	0		0	
East	PM Peak	6675	1-1	63.34	1-1	63.34
East	PM Peak	6826	0		0	
East	PM Peak	7009	2-1	71.53	2-1	71.53
East	PM Peak	7527	0		0	
East	PM Peak	8453	0		0	
East	PM Peak	8767	1-1	42.04	1-1	42.04
East	PM Peak	9106	0		0	
East	PM Peak	9165	1-1	47.27	1-1	47.27
East	PM Peak	9687	2-1	46.76	2-1	46.76
East	PM Peak	9703	1-1	31.11	1-1	31.11
East	PM Peak	9885	1-1	74.46	1-1	74.46
West	AM Peak	25	2-1	32.24	2-1	32.24
West	AM Peak	99	1-1	64.81	2-1	32.32

West	AM Peak	306	1-1	49.82	1-1	44.65
West	AM Peak	420	1-1	65.92	1-1	65.92
West	AM Peak	421	1-1	94.40	2-1	91.66
West	AM Peak	1300	0		0	
West	AM Peak	1766	1-1	53.05	1-1	56.52
West	AM Peak	1837	1-1	75.65	1-1	76.88
West	AM Peak	1839	0		0	
West	AM Peak	2697	2-1	75.75	2-1	75.75
West	AM Peak	3486	1-1	37.68	2-1	46.90
West	AM Peak	6017	1-1	55.56	1-1	55.56
West	AM Peak	6108	0		0	
West	AM Peak	6325	2-1	39.68	2-1	39.68
West	AM Peak	6328	1-1	63.87	2-1	61.84
West	AM Peak	6378	0		0	
West	AM Peak	7240	0		0	
West	AM Peak	7442	0		0	
West	AM Peak	7443	0		0	
West	AM Peak	7588	1-1	52.97	1-1	48.45
West	AM Peak	7624	1-1	44.94	2-1	66.03
West	AM Peak	7661	0		0	
West	AM Peak	7954	0		0	
West	AM Peak	8476	1-1	58.32	2-1	47.14
West	AM Peak	8712	0		0	
West	AM Peak	8897	1-1	71.03	1-1	71.03
West	Off Peak	75	0		0	
West	Off Peak	323	1-1	75.53	1-1	75.53
West	Off Peak	327	0		0	
West	Off Peak	941	1-1	81.36	1-1	80.72
West	Off Peak	1018	0		4-1	-27.56
West	Off Peak	1156	0		0	
West	Off Peak	1885	0		0	-19.18

West	Off Peak	2013	1-1	83.76	1-1	83.76
West	Off Peak	2244	1-1	84.78	1-1	84.78
West	Off Peak	2292	0		1-1	73.25
West	Off Peak	4403	1-1	91.31	1-1	91.31
West	Off Peak	4416	1-2	2.27	1-2	1.67
West	Off Peak	4594	1-1	37.30	1-1	30.51
West	Off Peak	5222	1-1	78.07	1-1	78.07
West	Off Peak	5230	0		0	
West	Off Peak	6300	2-1	70.71	2-1	70.71
West	Off Peak	6398	1-1	33.98	2-1	32.42
West	Off Peak	6449	0		0	-18.87
West	Off Peak	6661	0		4-1	-28.66
West	Off Peak	7126	1-1	82.69	1-1	82.69
West	Off Peak	7250	1-1	74.22	2-1	77.90
West	Off Peak	8170	0		0	
West	Off Peak	8213	1-1	37.56	1-1	22.29
West	Off Peak	8573	0		0	
West	Off Peak	8756	0		2-2	42.15
West	Off Peak	9146	1-1	91.93	1-1	91.93
West	Off Peak	9322	0		0	
West	Off Peak	6039	1-1	73.17	1-1	73.17
West	Off Peak	9713	1-1	51.85	1-1	51.85
West	PM Peak Ramp Closed	288	0		0	
West	PM Peak Ramp Closed	293	2-2	15.10	2-1	45.85
West	PM Peak Ramp Closed	1208	4-2	-6.15	4-2	-15.19
West	PM Peak Ramp Closed	1518	1-1	57.00	2-1	57.72
West	PM Peak Ramp Closed	1726	1-1	31.51	1-1	5.80
West	PM Peak Ramp Closed	2142	1-1	46.01	1-1	46.01
West	PM Peak Ramp Closed	2528	1-2	7.80	1-2	19.80
West	PM Peak Ramp Closed	2738	1-1	74.03	2-1	70.26
West	PM Peak Ramp Closed	2874	0		0	



West	PM Peak Ramp Closed	2889	0		0	16.80
West	PM Peak Ramp Closed	3049	4-1	-29.00	4-2	-20.46
West	PM Peak Ramp Closed	3452	0		0	
West	PM Peak Ramp Closed	3593	0		1-1	92.02
West	PM Peak Ramp Closed	3808	4-2	-12.08	4-2	-4.28
West	PM Peak Ramp Closed	4070	1-1	53.56	1-1	45.66
West	PM Peak Ramp Closed	4124	0		0	
West	PM Peak Ramp Closed	5176	0		0	
West	PM Peak Ramp Closed	5984	0		0	
West	PM Peak Ramp Closed	6613	1-1	29.33	1-1	126.50
West	PM Peak Ramp Closed	6843	1-1	55.32	2-1	46.74
West	PM Peak Ramp Closed	6865	1-1	37.60	1-1	11.02
West	PM Peak Ramp Closed	6949	3-1	-17.54	4-1	-54.49
West	PM Peak Ramp Closed	8016	4-2	-20.71	4-2	4.26
West	PM Peak Ramp Closed	8143	1-1	46.92	1-1	46.92
West	PM Peak Ramp Closed	8149	4-2	-28.13	4-2	-28.13
West	PM Peak Ramp Closed	8174	3-1	-25.90	3-1	-25.90
West	PM Peak Ramp Closed	8175	4-2	-32.64	4-2	-32.64
West	PM Peak Ramp Closed	8493	0		0	
West	PM Peak Ramp Open	900	0		4-1	-31.47
West	PM Peak Ramp Open	1652	0		0	
West	PM Peak Ramp Open	1788	0		0	
West	PM Peak Ramp Open	2635	3-1	-23.55	3-1	-23.55
West	PM Peak Ramp Open	2894	0		0	
West	PM Peak Ramp Open	3413	0		1-2	56.41
West	PM Peak Ramp Open	3854	3-1	-12.33	4-1	-8.87
West	PM Peak Ramp Open	5189	0		3-1	-13.22
West	PM Peak Ramp Open	5538	0		0	
West	PM Peak Ramp Open	5646	2-2	11.96	2-2	24.23
West	PM Peak Ramp Open	6133	0		1-2	5.19
West	PM Peak Ramp Open	6171	3-1	-14.51	4-1	-8.31

West	PM Peak Ramp Open	6174	0		0	
West	PM Peak Ramp Open	6274	1-1	37.11	1-1	64.44
West	PM Peak Ramp Open	6298	0		0	
West	PM Peak Ramp Open	6471	0		4-1	-27.79
West	PM Peak Ramp Open	6801	0		4-1	-14.80
West	PM Peak Ramp Open	6831	0		3-1	-17.29
West	PM Peak Ramp Open	7476	0		0	
West	PM Peak Ramp Open	7738	0		0	0.91
West	PM Peak Ramp Open	7740	4-2	-18.07	4-2	-18.07
West	PM Peak Ramp Open	8206	0		0	
West	PM Peak Ramp Open	8256	0		0	
West	PM Peak Ramp Open	8886	3-1	-22.80	3-1	-22.80
West	PM Peak Ramp Open	8923	4-2	-10.74	4-2	-10.74
West	PM Peak Ramp Open	9038	1-2	32.26	1-2	32.26
West	PM Peak Ramp Open	9042	1-1	32.79	2-1	33.19
West	PM Peak Ramp Open	9237	0		4-1	-29.07
West	PM Peak Ramp Open	9286	0		0	
West	PM Peak Ramp Open	9656	0		0	
West	PM Peak Ramp Open	9840	1-2	24.19	1-2	29.82

**TABLE A-2: Shock wave Types for Non-Crash Cases**

LANE	TIME PERIOD	CRASH ID	10 MINUTE		SHORT TERM	
			TYPE	SPEED	TYPE	SPEED
East	AM Peak	1185	2-1	50.17	2-1	50.17
East	AM Peak	1482	4-1	-16.85	4-1	-8.66
East	AM Peak	2224	4-1	-22.86	4-1	-37.04
East	AM Peak	3540	1-1	42.71	1-1	70.24
East	AM Peak	6278	1-2	12.26	2-2	20.05
East	AM Peak	6312	0		0	
East	AM Peak	7419	3-2	-15.30	3-2	-17.43
East	AM Peak	8165	2-1	44.32	2-1	33.72
East	AM Peak	8386	1-2	48.76	1-2	48.76
East	AM Peak	9280	1-1	59.36	1-1	59.36

East	Off Peak	161	4-2	-24.27	4-2	-24.27
East	Off Peak	169	1-1	66.47	1-1	66.47
East	Off Peak	450	1-1	95.74	1-1	95.74
East	Off Peak	547	2-1	67.27	2-1	67.27
East	Off Peak	1250	0		0	
East	Off Peak	1254	1-1	91.91	1-1	91.91
East	Off Peak	1866	0		0	
East	Off Peak	1936	0		0	
East	Off Peak	3647	3-2	-4.40	3-2	-4.40
East	Off Peak	5969	2-1	87.27	2-1	87.27
East	Off Peak	6235	2-1	82.45	2-1	80.35
East	Off Peak	6419	2-1	84.17	2-1	84.17
East	Off Peak	6928	0		4-2	-11.20
East	Off Peak	7125	0		0	
East	Off Peak	7349	1-1	63.45	1-1	63.45
East	Off Peak	7430	0		0	
East	Off Peak	7523	0		0	
East	Off Peak	7637	1-1	88.42	1-1	93.92
East	Off Peak	8675	0		0	
East	Off Peak	9307	2-1	91.14	2-1	94.56
East	Off Peak	9865	1-1	53.98	1-1	53.98
East	PM Peak	91	2-1	68.89	2-1	68.89
East	PM Peak	143	2-1	72.57	2-1	72.57
East	PM Peak	901	1-1	59.50	1-1	59.50
East	PM Peak	1285	2-1	66.88	2-1	83.34
East	PM Peak	1813	1-1	80.83	2-1	69.77
East	PM Peak	1978	0		0	
East	PM Peak	2019	2-1	47.43	1-1	18.24
East	PM Peak	3302	1-1	68.64	1-1	68.64
East	PM Peak	3801	1-1	56.21	1-1	56.21
East	PM Peak	5816	2-1	103.96	2-1	94.13
East	PM Peak	6167	2-1	73.68	2-1	73.68
East	PM Peak	6246	2-1	48.18	1-1	70.73
East	PM Peak	6293	2-1	92.88	2-1	92.88
East	PM Peak	6569	1-1	77.94	1-1	77.94
East	PM Peak	6675	0		4-2	-43.87
East	PM Peak	6826	2-1	58.34	2-1	58.34
East	PM Peak	7009	2-1	66.84	2-1	66.84
East	PM Peak	7527	3-2	-24.07	3-2	-24.07
East	PM Peak	8453	2-1	41.29	2-1	41.29
East	PM Peak	8767	2-1	60.44	2-1	40.01

East	PM Peak	9106	0		1-2	35.99
East	PM Peak	9165	0		0	
East	PM Peak	9687	2-1	85.11	2-1	85.11
East	PM Peak	9703	2-1	82.15	2-1	37.80
East	PM Peak	9885	1-1	95.10	1-1	95.10
West	AM Peak	25	1-1	50.10	1-1	67.09
West	AM Peak	99	2-1	80.28	2-1	78.33
West	AM Peak	306	1-1	38.95	1-1	38.95
West	AM Peak	420	1-1	91.13	2-1	110.88
West	AM Peak	421	1-1	90.78	1-1	85.62
West	AM Peak	1300	1-1	75.34	1-1	75.34
West	AM Peak	1766	1-1	77.27	1-1	73.93
West	AM Peak	1837	1-1	64.29	1-1	67.52
West	AM Peak	1839	2-1	69.52	2-1	69.52
West	AM Peak	2697	1-1	83.99	1-1	83.99
West	AM Peak	3486	2-1	48.30	2-1	48.30
West	AM Peak	6017	1-1	49.78	1-1	48.68
West	AM Peak	6108	2-1	62.02	2-1	69.77
West	AM Peak	6325	2-1	58.04	2-1	68.89
West	AM Peak	6328	1-1	54.53	1-1	54.53
West	AM Peak	6378	0		1-1	97.81
West	AM Peak	7240	0		4-1	-43.08
West	AM Peak	7442	2-1	38.94	2-1	38.94
West	AM Peak	7443	0		0	
West	AM Peak	7588	2-1	78.80	2-1	79.20
West	AM Peak	7624	1-1	70.47	1-1	81.75
West	AM Peak	7661	2-1	49.37	2-1	49.19
West	AM Peak	7954	1-1	81.49	2-1	80.93
West	AM Peak	8476	0		0	
West	AM Peak	8712	0		0	
West	AM Peak	8897	2-1	45.34	2-1	45.34
West	Off Peak	75	1-1	67.44	1-1	67.44
West	Off Peak	323	2-1	63.02	1-1	107.75
West	Off Peak	327	0		0	
West	Off Peak	941	1-1	86.91	1-1	86.91
West	Off Peak	1018	1-1	63.97	1-1	63.57
West	Off Peak	1156	0		0	
West	Off Peak	1885	0		0	
West	Off Peak	2013	1-1	78.68	1-1	82.08
West	Off Peak	2244	1-1	75.63	2-1	67.21
West	Off Peak	2292	1-1	73.21	1-1	75.80

West	Off Peak	4403	0		0	
West	Off Peak	4416	0		0	
West	Off Peak	4594	0		3-1	-14.63
West	Off Peak	5222	0		0	
West	Off Peak	5230	0		0	
West	Off Peak	6300	1-1	63.33	1-1	23.55
West	Off Peak	6398	2-1	70.75	2-1	70.75
West	Off Peak	6449	0		0	
West	Off Peak	6661	0		0	
West	Off Peak	7126	2-1	84.95	1-1	79.94
West	Off Peak	7250	1-1	78.03	1-1	78.03
West	Off Peak	8170	1-1	84.78	1-1	84.78
West	Off Peak	8213	1-1	81.82	1-1	78.57
West	Off Peak	8573	3-1	-11.75	3-1	-10.00
West	Off Peak	8756	0		4-1	-24.93
West	Off Peak	9146	1-1	95.95	1-1	95.95
West	Off Peak	9322	2-1	54.49	2-1	72.44
West	Off Peak	6039	1-1	83.12	1-1	87.90
West	Off Peak	9713	2-1	75.68	2-1	72.52
West	PM Peak Ramp Closed	288	1-1	71.74	1-1	71.74
West	PM Peak Ramp Closed	293	1-2	37.54	1-2	37.54
West	PM Peak Ramp Closed	1208	0		3-2	-2.50
West	PM Peak Ramp Closed	1518	2-1	54.42	2-1	58.76
West	PM Peak Ramp Closed	1726	0		3-1	-20.05
West	PM Peak Ramp Closed	2142	3-1	-17.34	3-1	-17.34
West	PM Peak Ramp Closed	2528	1-1	70.76	1-1	70.76
West	PM Peak Ramp Closed	2738	2-1	79.78	1-1	85.29
West	PM Peak Ramp Closed	2874	0		0	
West	PM Peak Ramp Closed	2889	2-2	32.69	1-2	32.96
West	PM Peak Ramp Closed	3049	1-1	67.31	1-1	69.16
West	PM Peak Ramp Closed	3452	0		0	
West	PM Peak Ramp Closed	3593	3-1	-23.38	3-1	-22.28
West	PM Peak Ramp Closed	3808	2-1	33.92	1-1	23.30
West	PM Peak Ramp Closed	4070	0		0	
West	PM Peak Ramp Closed	4124	0		0	
West	PM Peak Ramp Closed	5176	1-1	73.72	1-1	74.22
West	PM Peak Ramp Closed	5984	1-2	34.12	1-2	34.12
West	PM Peak Ramp Closed	6613	1-1	47.95	1-1	47.95
West	PM Peak Ramp Closed	6843	1-1	19.66	2-1	60.85
West	PM Peak Ramp Closed	6865	1-1	53.89	1-1	53.89
West	PM Peak Ramp Closed	6949	2-1	46.60	2-1	35.34

West	PM Peak Ramp Closed	8016	1-1	70.56	1-1	70.56
West	PM Peak Ramp Closed	8143	1-1	62.57	1-1	62.57
West	PM Peak Ramp Closed	8149	0		1-1	65.92
West	PM Peak Ramp Closed	8174	4-1	-37.04	4-1	-37.04
West	PM Peak Ramp Closed	8175	0		0	
West	PM Peak Ramp Closed	8493	0		0	
West	PM Peak Ramp Open	900	0		3-1	-88.86
West	PM Peak Ramp Open	1652	0		0	
West	PM Peak Ramp Open	1788	1-2	30.88	1-2	30.88
West	PM Peak Ramp Open	2635	1-2	49.38	1-2	49.38
West	PM Peak Ramp Open	2894	3-1	-18.10	4-1	-18.49
West	PM Peak Ramp Open	3413	0		3-1	-18.07
West	PM Peak Ramp Open	3854	4-1	-21.09	4-1	-19.99
West	PM Peak Ramp Open	5189	0		0	
West	PM Peak Ramp Open	5538	3-2	-10.98	4-2	-16.36
West	PM Peak Ramp Open	5646	4-1	-13.82	0	
West	PM Peak Ramp Open	6133	0		0	
West	PM Peak Ramp Open	6171	1-2	22.77	1-2	28.86
West	PM Peak Ramp Open	6174	0		0	
West	PM Peak Ramp Open	6274	0		0	
West	PM Peak Ramp Open	6298	1-1	89.91	1-1	89.91
West	PM Peak Ramp Open	6471	4-1	-19.74	4-1	-8.66
West	PM Peak Ramp Open	6801	2-2	1.17	2-2	41.92
West	PM Peak Ramp Open	6831	0		4-1	-9.66
West	PM Peak Ramp Open	7476	3-1	-15.27	3-1	-19.41
West	PM Peak Ramp Open	7738	0		0	
West	PM Peak Ramp Open	7740	0		3-1	-6.12
West	PM Peak Ramp Open	8206	3-1	-14.78	0	
West	PM Peak Ramp Open	8256	2-2	20.80	2-1	48.95
West	PM Peak Ramp Open	8886	3-2	-5.36	4-1	-8.85
West	PM Peak Ramp Open	8923	0		0	
West	PM Peak Ramp Open	9038	2-2	43.99	2-1	70.96
West	PM Peak Ramp Open	9042	0		0	
West	PM Peak Ramp Open	9237	0		0	
West	PM Peak Ramp Open	9286	4-2	-14.41	1-1	38.65
West	PM Peak Ramp Open	9656	1-1	74.81	1-1	74.21
West	PM Peak Ramp Open	9840	0		0	

## VITA AUCTORIS

<b>Name</b>	Steven Volpatti
<b>Place of Birth</b>	Windsor, Ontario, Canada
<b>Year of Birth</b>	1984
<b>Education</b>	St. Anne Secondary School Tecumseh, Ontario, Canada 1998-2003  University of Windsor Windsor, Ontario, Canada B.A.Sc. Civil Engineering (Co-op) 2003-2007  University of Windsor Windsor, Ontario, Canada M.A.Sc. Civil Engineering 2007-2009
<b>Conferences</b>	Presentation: ITS Canada Annual Conference and General Meeting 2009 Paper Submitted: Transportation Research Board Annual Meeting 2010
<b>Membership</b>	Professional Engineers of Ontario Engineer in Training